Supporting Information for

# Mimicking the Constrained Geometry of a Nitrogen-Fixation Intermediate

Tianchang Liu, Michael R. Gau, and Neil C. Tomson*

*P. Roy and Diana T. Vagelos Laboratories, Department of Chemistry,*
*University of Pennsylvania, Philadelphia, Pennsylvania, 19104, United States*

## Table of Contents

1. Experimental Details and Characterization Data for All New Compounds ..... S2
2. Summary of Crystallographic Data and Comparison to the Literature ..... S6
3. Spectroscopic Data ..... S11
4. Electrochemistry Data ..... S20
5. Computational Details ..... S21
6. DFT-optimized Atomic Coordinates ..... S23
7. References ..... S26

## Experimental Details and Characterization Data for All New Compounds

**General Methods.** All reactions involving transition metals were performed under an inert atmosphere of $N_2$ either in a PureLab HE glovebox or using standard Schlenk line technique. Glassware, stir bars, filter aid (Celite) and 4Å molecular sieves were dried in an oven at 150 °C for at least 12 h prior to use. All solvents (*n*-pentane, *n*-hexane, diethyl ether, fluorobenzene, THF) were dried by passage through a column of activated alumina, deoxygenated by sparging with $N_2$ for 15 min, and stored over 4Å molecular sieves. Deuterated solvents were purchased from Cambridge Isotope Laboratories, Inc., and dried over Na/benzophenone ($C_6D_6$, THF-$d_8$), distilled and stored under $N_2$ over activated 4Å molecular sieves. $^{15}N_2$ (98 atom % $^{15}N$) was purchased from MilliporeSigma and used without further purification. ($^3$PDI$_2$)Sr(OTf)$_2$,[1] [($^3$PDI$_2$)Fe$_2$(PPh$_3$)$_2$Cl][OTf] (**$^{Ph}$[Fe$_2$Cl]$^+$**),[2] [($^3$PDI$_2$)Fe$_2$(PMe$_3$)$_2$Cl][OTf] (**$^{Me}$[Fe$_2$Cl]$^+$**)[3] was synthesized according to literature procedures. $KC_8$ was synthesized according to literature procedures and stored at -35 °C in a glovebox prior to use.[4] $PPh_3$ was purchased from MilliporeSigma, purified by recrystallization from hot ethanol and dried under vacuum (30 mbar) at 40 °C for 6 h prior to use.[5] $PMe_3$ (98%) was either purchased from Strem Chemicals or synthesized according to literature procedures and stored as a 1 M solution in THF at -35 °C under dry nitrogen in a glovebox.[6] 1,3,5-trimethoxybenzene was purchased from Alfa Aesar, recrystallized twice from *n*-hexane, followed by drying under vacuum (30 mbar) at 60 °C for 10 h prior to use.[5] [$^n$Bu$_4$N][$PF_6$] (98%) was purchased from MilliporeSigma and recrystallized twice from hot ethanol, followed by drying at 60 °C under 30 mbar for 10 h prior to use.[5] Anhydrous $FeCl_2$ was purchased from Strem Chemicals and used without further purification. $^1$H, $^2$H, $^{13}$C{$^1$H}, $^{31}$P{$^1$H}, $^{15}$N{$^1$H}, $^1$H-$^{13}$C HSQC and $^1$H-$^1$H COSY NMR spectra were recorded on Bruker DMX 360, UNI 400, AV3BIO 500, UNI 500 or NEO 600 spectrometers. All chemical shifts ($\delta$) are reported in units of ppm, with references to the residual protio-solvent resonance for proton and carbon chemical shifts. External $H_3PO_4$ and $CH_3NO_2$ were used for referencing $^{31}$P and $^{15}$N NMR chemical shifts, respectively. Elemental analysis was performed by Midwest Microlab, LLC. IR samples were prepared as KBr pellets using powdered KBr that had been dried under vacuum at 130 °C for 4 h. The water detected by IR spectroscopy as a wide band at 3440 cm$^{-1}$ results from atmospheric hydration of the surface of the pellet in the 50-60 sec between removal of the sample from an inert atmosphere and the collection of IR data on a JASCO FT/IR-480 Plus spectrometer.

**X-ray Crystallography.** Single-crystal X-ray diffraction data were collected on a Rigaku XtaLAB Synergy-S HPC area detector (Dectris PILATUS3 R 200K) diffractometer with graphite-monochromated Mo Kα radiation (λ = 0.71073 Å) at 100 K.[7] Rotation frames were integrated using SAINT,[8] producing a listing of unaveraged $F^2$ and $\sigma(F^2)$ values. The intensity data were corrected for Lorentz and polarization effects and for absorption using either SADABS (**$^{Me}$[Fe$_2$N$_2$]$^0$**) or SCALE3 ABSPACK (**$^{Ph}$[Fe$_2$N$_2$]$^0$**).[9,10] The structures were solved by direct methods by

using SHELXT and refined by full-matrix least squares, based on $F^2$ using SHELXL-2018. Crystal parameters and refinement results are given in Table S1 and Table S2.

**Computational Methods.** Density functional theory (DFT) calculations were performed with the ORCA program package, *v*3.0.3.[11] The geometry optimization was carried out at the B97-D3 level of DFT,[12] using a model compound derived from crystallographic data, with the *p*-$^t$Bu groups truncated to hydrogens. The def2-TZVP basis sets and the def2-TZVP/J auxiliary basis sets (used to expand the electron density in the resolution-of-identity (RI) approach) were used for Fe, P, and N.[13] All other atoms were described using the def2-SV(P) basis sets and def2-SV/J auxiliary basis sets. The SCF calculations were tightly converged ($1x10^{-8}$ $E_h$ in energy, $1x10^{-7}$ $E_h$ in the density change, and $5x10^{-7}$ in the maximum element of the DIIS error vector). The geometry was considered converged after the energy change was less than $1x10^{-6}$ $E_h$, the gradient norm and maximum gradient element were smaller than $3x10^{-4}$ $E_h$-Bohr$^{-1}$ and $1x10^{-4}$ $E_h$-Bohr$^{-1}$, respectively, and the root-mean square and maximum displacements of all atoms were smaller than $6x10^{-4}$ Bohr and $1x10^{-3}$ Bohr, respectively. A numerical frequency calculation was used to verify that the calculated structure represented a local minimum on the potential energy surface. The reported energy is a Gibbs free energy, calculated for 298.15 K and 1.00 atm, as obtained from the numerical frequency calculation on the optimized geometry. Plots were generated using the program Chimera,[14] with isosurface cutoffs of |0.025| a.u.

**Electrochemistry.** Cyclic voltammetry experiments were performed using a BASi C3 Cell Stand paired with an Epsilon E2 Potentiostat. The data were processed with BASi Epsilon-EC software version 2.13.77. All experiments were performed under an $N_2$ atmosphere in a VAC OMNI-LAB glovebox using an electrochemical cell that consists of a glassy carbon (3 mm outer diameter) working electrode, a platinum wire counter electrode and a $AgPF_6$ (100 mM in THF)/Ag reference electrode. All experiments were conducted in THF, with 1 mM analyte and 100 mM [$^n$Bu$_4$N][$PF_6$] as the supporting electrolyte. Potentials were reported *versus* $Cp_2Fe^{+/0}$, which was added as an internal standard for reference at the end of each experiment.

**Synthesis of ($^3$PDI$_2$)Fe$_2$($\mu$-N$_2$)(PPh$_3$)$_2$ ($^{Ph}$[Fe$_2$N$_2$]$^0$).** A $KC_8$ (28.9 mg, 0.22 mmol) suspension in THF was chilled to -35 °C, then added dropwise to a pre-chilled, stirred solution of $^{Ph}$[Fe$_2$Cl]$^+$ (144 mg, 0.11 mmol) in 10 mL THF, resulting in a rapid color change from dark brown to purplish red. The mixture was allowed to warm to room temperature and stirred for 1 hour. All volatile materials were then removed under vacuum. The residue was treated with 5 mL $Et_2O$, then filtered through Celite and stored at -35 °C for three days to afford $^{Ph}$[Fe$_2$N$_2$]$^0$ as dark red needles. Yield 48.0 mg (35 %). Analytically pure material was obtained following recrystallization under the same conditions. $^1$H NMR (600 MHz, THF-$d_8$, 298 K): $\delta$ = 7.69 (s, 4H, py *m*-*H*), 7.16 (t, $^3J_{HH}$ = 9.3 Hz, 6H, Ar*H*), 7.07 (t, $^3J_{HH}$ = 8.4 Hz, 12H, Ar*H*), 6.79 (t, $^3J_{HH}$ = 9.3 Hz, 12H, Ar*H*), 4.39 – 4.34 (m, 4H, C$H_2$), 3.86 – 3.82 (m, 4H, C$H_2$), 2.46 – 2.38 (m, 2H, C$H_2$), 2.13 (d, $^5J_{PH}$ = 5.4 Hz, 12H, C$H_3$), 1.35 (s, 18H, C(C$H_3$)$_3$), 0.32 – 0.27 (m, 2H, C$H_2$) ppm; $^{13}$C{$^1$H} NMR (600 MHz, THF-$d_8$, 298 K): $\delta$ = 145.88 (d, $^3J_{PC}$ = 15.6 Hz, Ar*C*), 141.83 (d, $^3J_{PC}$ = 21 Hz, $C_{imine}$), 137.75 (s, Ar*C*), 109.76 (s, Ar*C*), 61.10 (s, *C*H$_2$), 42.04 (t,

$^4J_{PC}$ = 30 Hz, *C*H$_2$), 35.68 (s, *C*(CH$_3$)$_3$), 32.39 (s, C(*C*H$_3$)$_3$), 15.90 (d, $^2J_{PC}$ = 68.4 Hz, P(*C*H$_3$)$_3$), 13.93 (d, $^2J_{PC}$ = 11.4 Hz, *C*H$_3$) ppm; $^{31}$P{$^1$H} NMR (500 MHz, THF-$d_8$, 298 K): $\delta$ = 60.97 (s, *P*(CH$_3$)$_3$) ppm. FT-IR (KBr pellet): $\nu_{N\text{-}N}$ = 1959 cm$^{-1}$. Anal. Calcd. for $C_{68}H_{76}Fe_2N_8P_2$•2$C_4H_8O$ (1327.27 g/mol): C, 68.77; H, 7.29; N, 8.44. Found: C, 68.14; H, 7.00; N, 8.77.

**Alternative synthesis of ($^3$PDI$_2$)Fe$_2$($\mu$-N$_2$)(PPh$_3$)$_2$ ($^{Ph}$[Fe$_2$N$_2$]$^0$).** To a stirred solution of ($^3$PDI$_2$)Sr(OTf)$_2$ (200 mg, 0.222 mmol) in THF (7 mL) was added solid, anhydrous FeCl$_2$ (56.4 mg, 0.444 mmol) at room temperature. After being stirred for 2 h, the purple slurry was treated with PPh$_3$ (116.4 mg, 0. 444 mmol). The reaction mixture was stirred for an additional 10 min, then chilled to -35 °C. A suspension of KC$_8$ (60 mg, 0.444 mmol) in THF (2 mL) was chilled to -35 °C and added into the reaction mixture. The resulting dark green slurry was allowed to warm to room temperature and stirred for 1 h, during which time the color gradually turned dark brown. The reaction mixture was filtered through Celite, then chilled again to -35 °C. A second portion of KC$_8$ (60 mg, 0.444 mmol) in THF (2 mL) was chilled to -35 °C and added into the reaction mixture. The reaction mixture was allowed to warm to room temperature and stirred for 1 h, during which time the slurry gradually turned purplish red. The volatile materials were removed under reduced pressure. The solid residue was extracted with 7 mL of diethyl ether, filtered through Celite, concentrated to 3 mL, filtered again through Celite and stored at -35 ºC for 3 d to afford $^{Ph}$[Fe$_2$N$_2$]$^0$ as dark red needles. Yield 44 mg (17.4 %). The material obtained by this method displayed the same analytical data as those given above.

**Synthesis of [($^3$PDI$_2$)Fe$_2$($\mu$-$^{15}$N$_2$)(PPh$_3$)$_2$] ($^{Ph}$[Fe$_2$$^{15}$N$_2$]$^0$).** The synthesis of $^{Ph}$[Fe$_2$$^{15}$N$_2$]$^0$ was prepared according to the general procedure given above for the alternative synthesis of $^{Ph}$[Fe$_2$N$_2$]$^0$, but with the following modifications. The dark brown slurry obtained following the initial addition of KC$_8$ was added to a 100 mL Schlenk flask. The flask was cooled using a dry ice/acetone both, then evacuated for *ca*. 1 min and refilled with Ar; this procedure was repeated two times. The flask was then charged with a sealed glass capsule containing the second portion of KC$_8$. After resealing the flask and evacuating it for 1 min, the headspace was refilled with *ca*. 1 atm of $^{15}$N$_2$. The glass capsule was broken with vigorous stirring, then the flask was allowed to warm to 0 °C and stirred for 30 min. The color of the solution turned from brown to red on warming. The mixture was then allowed to obtain room temperature and stirred for 1 h before workup, as described above. Yield 40.7 mg (15.5 % on 0.222 mmol scale). $^{15}$N NMR (61 MHz, THF-$d_8$, 25 °C): $\delta$ = 355.2 (s, Fe$_2$$^{15}$*N*$_2$) ppm. The product was determined to be 93 % pure by comparison with an internal standard of 1,3,5-trimethoxybenzene. FT-IR (KBr pellet): $\nu_{15N\text{-}15N}$ = 1896 cm$^{-1}$.

**Synthesis of ($^3$PDI$_2$)Fe$_2$($\mu$-N$_2$)(PMe$_3$)$_2$ ($^{Me}$[Fe$_2$N$_2$]$^0$).** A solution of $^{Me}$[Fe$_2$Cl]$^+$ (109 mg, 0.08 mmol) in THF (10 mL) was chilled to -35 ºC. A slurry of KC$_8$ (30 mg, 0.222 mmol) in THF (2 mL) was also chilled to -35 °C, then slowly added the reaction mixture, resulting in a rapid color change from dark brown to red. The mixture was allowed to warm to room temperature and stirred for 1 hour. All volatile materials were then removed under reduced pressure. The reaction mixture was then extracted with 5 mL Et$_2$O, filtered through Celite and stored at -35 ºC for three days to afford

**$^{Me}$[Fe$_2$N$_2$]$^0$** as dark red needles. Yield 10.1 mg (11 %). Following recrystallization under the conditions described above, spectroscopically pure material was obtained, as determined by $^1$H NMR spectroscopy in the presence of an internal standard. $^1$H NMR (600 MHz, THF-$d_8$, 298 K): $\delta$ = 7.77 (s, 4H, py *m-H*), 5.09 – 5.05 (m, 4H, C$H_2$), 4.53 – 4.45 (m, 4H, C$H_2$), 2.66 – 2.62 (m, 2H, C$H_2$), 2.39 (d, $^5J_{PH}$ = 5.4 Hz, 12H, C$H_3$), 1.38 (s, 18H, C(C$H_3$)$_3$), 0.59 (d, $^2J_{PH}$ = 7.2 Hz, 18H, P(C$H_3$)$_3$), 0.46 – 0.41 (m, 2H, C$H_2$) ppm; $^{13}$C{$^1$H} NMR (600 MHz, THF-$d_8$, 298 K): $\delta$ = 145.88 (d, $^3J_{PC}$ = 15.6 Hz, Ar*C*), 141.83 (d, $^3J_{PC}$ = 21 Hz, $C_{imine}$), 137.75 (s, Ar*C*), 109.76 (s, Ar*C*), 61.10 (s, *C*H$_2$), 42.04 (t, $^4J_{PC}$ = 30 Hz, *C*H$_2$), 35.68 (s, *C*(CH$_3$)$_3$), 32.39 (s, C(*C*H$_3$)$_3$), 15.90 (d, $^2J_{PC}$ = 68.4 Hz, P(*C*H$_3$)$_3$), 13.93 (d, $^2J_{PC}$ = 11.4 Hz, *C*H$_3$) ppm; $^{31}$P{$^1$H} NMR (500 MHz, THF-$d_8$, 298 K): $\delta$ = 22.33 (s, *P*(CH$_3$)$_3$) ppm. FT-IR (KBr pellet): $\nu_{Ns\text{-}N}$ = 2003 cm$^{-1}$. **$^{Me}$[Fe$_2$N$_2$]$^0$** was observed to undergo slow thermal decomposition, which prevented the collection of suitable microanalytical data.

## Summary of Crystallographic Data

**Table S1**. Summary of crystallographic data for compounds reported in this work.

| Complexes | $^{Ph}[Fe_2N_2]^0$ •2$Et_2O$ | $^{Me}[Fe_2N_2]^0$ •$Et_2O$•$^1/_2$ Pentane |
|---|---|---|
| Empirical formula | $C_{76}H_{96}Fe_2N_8O_2P_2$ | $C_{45}H_{81}Fe_2N_8OP_2$ |
| Formula weight | 1327.27 | 923.81 |
| Temperature/K | 100 | 100 |
| Crystal system | triclinic | triclinic |
| Space group | P-1 | P-1 |
| a/Å | 10.6831(2) | 9.8631(6) |
| b/Å | 16.4143(4) | 13.0959(8) |
| c/Å | 20.2856(4) | 20.1607(12) |
| α/° | 91.674(2) | 91.874(2) |
| β/° | 98.0110(10) | 92.340(2) |
| γ/° | 98.486(2) | 106.816(2) |
| Volume/Å$^3$ | 3479.41(13) | 2487.9(3) |
| Z | 2 | 2 |
| $\rho_{calc}$/g•cm$^{-3}$ | 1.267 | 1.233 |
| μ/mm$^{-1}$ | 0.515 | 0.688 |
| F(000) | 1412.0 | 994.0 |
| Crystal size/mm$^3$ | 0.34 × 0.12 × 0.04 | 0.27 × 0.23 × 0.17 |
| Radiation | Mo $K_\alpha$ (λ = 0.71073) | Mo $K_\alpha$ (λ = 0.71073) |
| 2$\theta$ range for data collection | 4.06 - 55.142° | 5.048 to 55.096° |
| Index ranges | -13 ≤ h ≤ 13<br>-21 ≤ k ≤ 21<br>-26 ≤ l ≤ 26 | -12 ≤ h ≤ 12<br>-16 ≤ k ≤ 17<br>-26 ≤ l ≤ 26 |
| Reflections collected | 127175 | 52187 |
| Independent reflections | 26672 [$R_{int}$ = 0.070] | 11406 [$R_{int}$ = 0.0413] |
| Data/restraints/parameters | 26672/0/826 | 11406/0/542 |
| Goodness-of-fit on $F^2$ | 1.029 | 1.111 |
| Final R indexes [I>=2σ (I)] | $R_1$ = 0.0557, $wR_2$ = 0.1431 | $R_1$ = 0.0440, $wR_2$ = 0.1000 |
| Final R indexes [all data] | $R_1$ = 0.0672, $wR_2$ = 0.1501 | $R_1$ = 0.0603, $wR_2$ = 0.1063 |
| Largest diff. peak/hole / e•Å$^{-3}$ | 0.87/-0.47 | 0.71/-0.53 |

**Table S2**. Selected bond lengths (Å) and angles (°) for experimental and DFT computational data.

| | $^{Ph}[Fe_2N_2]^0$ (XRD) | $^{Me}[Fe_2N_2]^0$ (XRD) | $^{Me}[Fe_2N_2]^0$ (DFT) |
|---|---|---|---|
| **Fe–Fe** | 4.5628(6) | 4.6066(6) | 4.536 |
| **Fe–$N_{N2}$** | 1.835(3) | 1.828(2) | 1.802 |
| | 1.823(3) | 1.811(2) | 1.802 |
| **Fe–$N_{imine}$** | 1.918(3) | 1.902(2) | 1.962 |
| | 1.924(3) | 1.910(2) | 1.962 |
| | 1.921(3) | 1.911(2) | 1.963 |
| | 1.926(3) | 1.909(2) | 1.964 |
| **Fe–$N_{py}$** | 1.830(3) | 1.814(2) | 1.857 |
| | 1.831(3) | 1.822(2) | 1.858 |
| **$N_\mu$–$N_\mu$** | 1.139(3) | 1.135(3) | 1.148 |
| **$N_{imine}$–$C_{imine}$** | 1.333(4) | 1.345(3) | 1.350 |
| | 1.338(4) | 1.339(3) | 1.350 |
| | 1.338(4) | 1.343(3) | 1.350 |
| | 1.339(4) | 1.340(3) | 1.350 |
| **$C_{imine}$–$C_{py}$** | 1.420(4) | 1.426(3) | 1.437 |
| | 1.428(4) | 1.424(3) | 1.437 |
| | 1.429(4) | 1.422(3) | 1.438 |
| | 1.428(4) | 1.430(3) | 1.438 |
| **∠Fe–$N_\mu$–$N_\mu$** | 159.8(3) | 157.99(19) | 160.0 |
| | 163.2(3) | 162.88(19) | 160.1 |
| **Δ** | 0.067 | 0.061 | 0.064 |

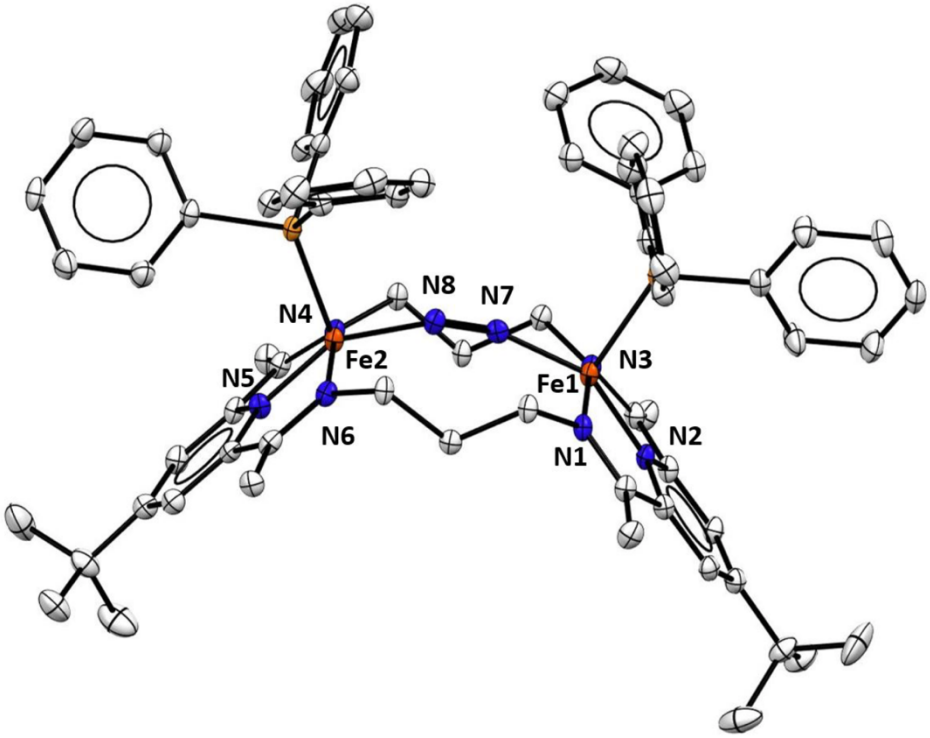


**Figure S1**. Crystal structure of $^{Ph}[Fe_2N_2]^0$, with thermal ellipsoids at the 50% probability level. The co-crystallized solvent molecules and hydrogen atoms were omitted for clarity.

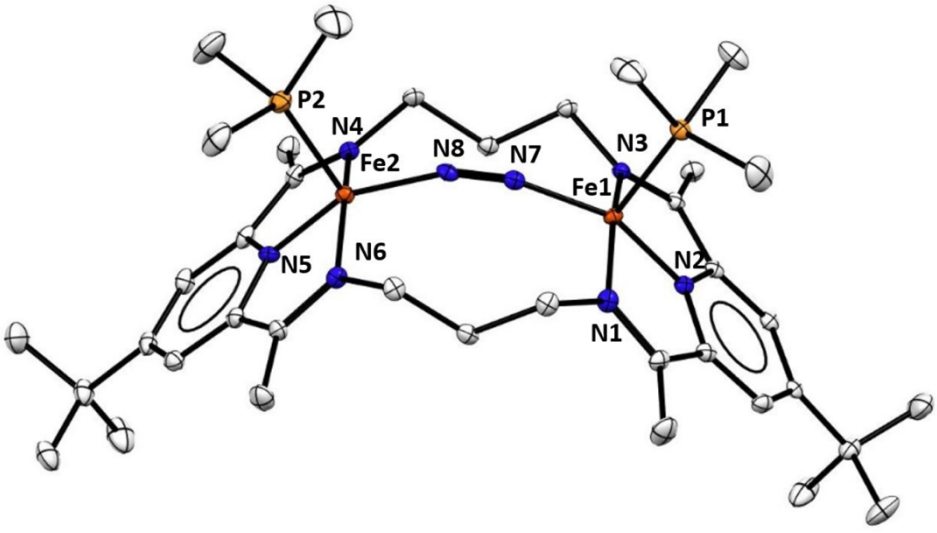


**Figure S2**. Crystal structure of $^{Me}[Fe_2N_2]^0$, with thermal ellipsoids at the 50% probability level. The co-crystallized solvent molecules and hydrogen atoms were omitted for clarity.

**Table S3.** Dinitrogen N–N bond lengths and stretching frequencies of neutral, diiron bridging dinitrogen compounds (top) and other species with non-linear M–$N_2$–M bridges (bottom).

| complex | N–N (Å) | $\nu_{NN}$ ($cm^{-1}$) | ref |
|---|---|---|---|
| [Fe(carb-PNP)]$_2$($\mu$-$N_2$) | 1.106(4) | | 16 |
| [($\eta^6$-$C_6H_6$)Fe($Me_2SiC_6H_4SiMe_2$)]$_2$($\mu$-$\eta^1$:$\eta^1$-$N_2$) | 1.119(3) | 2035[b] | 17 |
| {[$PhBP^{CH2Cy}_3$]Fe(OAc)}$_2$($\mu$-$N_2$) | 1.120(5) | 2083[a] | 18 |
| [{Fe(N,arene-Piso)}$_2$($\mu$-$N_2$)] | 1.124(6) | 2005[b] | 19 |
| [($\eta^6$-$C_6H_5Me$)Fe($Me_2SiC_6H_4SiMe_2$)]$_2$($\mu$-$\eta^1$:$\eta^1$-$N_2$) | 1.126(3) | 2022[b] | 17 |
| [(FeH($PP_3$))($\mu$-$N_2$)(Fe($PP_3$))][$BPh_4$] | 1.127(2) | | 20 |
| [Cp*($Ph_2PC_6H_4S$)Fe]$_2$($\mu$-$N_2$) | 1.130(6) | 2016[a] | 21 |
| [Fe(CO)$_2$($P(OCH_3)_3$)$_2$](μ-$N_2$) | 1.13 | | 22 |
| [Fe(PNNP-Cy)]$_2$($\mu$-$N_2$) | 1.134(6) | | 23 |
| [Fe(CO)$_2$($PEt_3$)$_2$]($\mu$-$N_2$) | 1.134(21) | | 24 |
| **$^{Me}$[$Fe_2N_2$]$^0$** | **1.135(3)** | **2003[a]** | **this work** |
| [Fe(PNNP-Ph)]$_2$($\mu$-$N_2$) | 1.135(4) | | 23 |
| {[$PhBP^{iPr}_3$]Fe}$_2$($\mu$-$N_2$) | 1.138(6) | | 25 |
| [($SiP_2S$)- Fe]$_2$($\mu$-$N_2$) | 1.138(2) | 1888[a] | 26 |
| **$^{Ph}$[$Fe_2N_2$]$^0$** | **1.139(3)** | **1959[a]** | **this work** |
| [($\eta^6$-$C_6H_3Me_3$)Fe($Me_2SiC_6H_4SiMe_2$)]$_2$($\mu$-$\eta^1$:$\eta^1$-$N_2$) | 1.139 | 2012[b] | 27 |
| [($^{Me}$CNC)Fe($N_2$)]$_2$($\mu$-$N_2$) | 1.140 | | 28 |
| [Fe(dmpe)$_2$]$_2$($\mu$-$N_2$) | 1.144(3) | 1933[b] | 29 |
| [Fe(AltraPhos)]$_2$($\mu$-$N_2$) | 1.146(7) | 2010[a] | 30 |
| [$P_2^{P'Ph}$Fe(H)]$_2$($\mu$-$N_2$) | 1.15 | | 31 |
| ([$N_2P_2$]Fe)$_2$($\mu$-$N_2$) | 1.166(3) | 1760[a] | 32 |
| [{Fe(Me-$PNP^{\alpha H}$)}$_2$($\mu$-$N_2$)][($BAr^F_4$)$_2$] | 1.170(5) | | 33 |
| ($^{iPr}$DPB)Fe($\mu$-1,2-$N_2$)Fe($^{iPr}$DPB) | 1.170(5) | | 34 |
| Fe(depe)$_2$($\mu$-$N_2$)Fe($^i$$Pr_2$Tp)($BAr^F_4$) | 1.177(5) | 1825[a] | 35 |
| ($Tp^{Ph,\ Me}$Fe)$_2$($\mu$-$N_2$) | 1.1804(19) | 1779[b] | 36 |
| L$^{t\text{Bu}}$Fe($\mu$-$N_2$)FeL$^{t\text{Bu}}$ | 1.182(5) | 1778[b] | 37 |
| ([$^{CY5}$NpN$^{Me,\ Me'}$]Fe)$_2$($\mu$-$N_2$) | 1.183(6) | | 38 |
| [$Tp^{tBu,Me}$Fe]$_2$($\mu$-$\eta^1$:$\eta^1$-$N_2$) | 1.184(7) | | 39 |
| ([$^{CY5}$NpN$^{iPr,\ iPr'}$]Fe)$_2$($\mu$-$N_2$) | 1.186(3) | | 38 |
| [Fe(NpNP$^{iPr}$)]$_2$($\mu$-$N_2$) | 1.186(5) | 1755[a] | 40 |
| [(2,6-$Me_2Ph$)$_2$nacnacCr($\mu$-$N_2$)(THF)]$_3$ | 1.158(4) | 2244[a] | 41 |
| | 1.168(4) | 2124[a] | |
| {[($^{Ar}$PDI)Cr- (THF)]$_2$($\mu$-$N_2$)} | 1.241(6) | | 42 |
| [($^{Ar}$PDI)V]$_2$($\mu$-$N_2$) | 1.259(6) | | 43 |
| [($^{Ar'}$PDI)V]$_2$($\mu$-$N_2$) | 1.242(5) | | 43 |
| [$\eta_5$-$C_5Me_5$)Zr]$_2$[$\mu_2$-$\eta_2$,$\eta_2$-4,5-($\eta_5$ -$C_9H_5$-1-(*i*Pr)-3-(Me))}$_2$]($\mu_2$-$\eta_1$,$\eta_1$ -$N_2$) | 1.197(3) | 1563[a] | 44 |
| α-$N_2$ intermediate on Fe(111) surface | 1.29 | 1490[a] | 45, 46 |

[a] Measured by IR spectroscopy. [b] Measured by resonance Raman spectroscopy.

**Table S4.** Dinitrogen N–N bond lengths and stretching frequencies of PDI-bound iron dinitrogen compounds.

| complex | N–N (Å) | $\nu_{NN}$ ($cm^{-1}$) | ref |
|---|---|---|---|
| ($^{iPr}$PDI)Fe(THT)($N_2$) | 1.085 | 2045[a] | 47 |
| ($^{Ar}$PDI)Fe($\mu$,$\eta_2$-$N_2$)Na(THF) | 1.090(5) | | 48 |
| ($^{iPr}$PDI)Fe($N_2$)$_2$ | 1.090(2) | 2124[a] | 49 |
| | 1.104(3) | 2053[a] | |
| (4-$Me_2N$-$^{iPr}$PDI)Fe($N_2$)$_2$ | 1.100 | 2034[a] | 50 |
| | 1.133 | | |
| (4-$^{t}$Bu-$^{iPr}$PDI)Fe($N_2$)$_2$ | 1.112 | | 50 |
| | 1.107 | 2041[a] | |
| ($^{iPr}$PhPDI)Fe($N_2$)$_2$ | 1.106(6) | 2138[a] | 51 |
| | 1.107(5) | 2086[a] | |
| ($^{iPr}$PDI)Fe($PEt_3$)($N_2$) | 1.111 | 2028[a] | 47 |
| ($^{iPr}$EtPDI)Fe$N_2$ | 1.112(2) | 2027[a] | 52 |
| ($^{iPr}$iPrPDI)Fe$N_2$ | 1.117(5) | 2026[a] | 52 |
| [($^{iPr,Et}$PDI)Fe$N_2$]$_2$($\mu_2$-$N_2$) | | 2075[a] | 53 |
| | | 2090[a] | |
| [($^{Me}$BPDI)Fe($N_2$)]$_2$($\mu_2$-$N_2$) | 1.123(3) | | 54 |
| [($^{Et}$PDI)Fe($N_2$)]$_2$($\mu_2$-$N_2$) | 1.124(3) | | 54 |
| [($^{iPr}$PDI)Fe($C_6H_5$)$N_2$]Li($Et_2O$)$_3$ | | 2069[a] | 55 |
| **$^{Me}$[$Fe_2N_2$]$^0$** | **1.135(3)** | **2003[a]** | **this work** |
| [$^{iPr}$BIPFe($N_2$)($CH_2CH_2Ph$)][MgX-($THF$)$_5$] | 1.137(10) | | 56 |
| [Li($OEt_2$)$_3$]-[($^{iPr}$PDI)Fe($CH_2CMe_3$)($N_2$)] | 1.138(3) | 1948[a] | 57 |
| [($^{iPr}$PDI)Fe($C_6H_4$-*p*-$CH_3$)$N_2$]Li($Et_2O$)$_3$ | 1.138(3) | 2068[a] | 55 |
| **$^{Ph}$[$Fe_2N_2$]$^0$** | **1.139(3)** | **1959[a]** | **this work** |
| ($^{Ar}$PDI)Fe($\mu$-$N_2$)Na($Et_2O$)$_3$ | 1.154(6) | | 48 |

[a] Measured by IR spectroscopy.

**Table S5.** Dinitrogen N–N bond lengths and stretching frequencies of alkali metal-containing diiron dinitrogen compounds.

| complex | N–N (Å) | $\nu_{NN}$ ($cm^{-1}$) | ref |
|---|---|---|---|
| [([PhBP$^{iPr}_3$]Fe)$_2$($\mu$-$N_2$)][Na($THF$)$_6$] | 1.171(4) | | 58 |
| [L$^{Me}$Fe($\mu$-$N_2$)FeL$^{Me}$][K(18-crown-6)($THF$)$_2$] | 1.186(6) | 1749[a] | 59 |
| [L$^{Me}$FeNNL$^{Me}$][K(18-crown-6)(12-crown-4)]$_2$ | 1.190(8) | 1738[a] | 60 |
| $Rb_2$[LFe($\mu$-$N_2$)]$_3$ | 1.191(14) | | 61 |
| $Cs_2$[LFe($\mu$-$N_2$)]$_3$ | 1.199 | | 61 |
| $K_2$[L$^{tBu}$FeNNFeL$^{tBu}$] | 1.233(6) | 1589[a] | 62 |
| $Cs_2$[LFe($\mu$-Cl)($\mu$-$N_2$)$_2$] | 1.234(11) | | 61 |
| $Na_2$[L$^{Me}$FeNNFeL$^{Me}$] | 1.253(6) | 1612[a] | 63 |
| $Rb_2$[L$^{Me}$FeNNFeL$^{Me}$] | 1.257(8) | 1621[a] | 63 |
| $Cs_2$[L$^{Me}$FeNNFeL$^{Me}$] | 1.33(2) | 1613[a] | 63 |

[a] Measured by IR spectroscopy.

## Spectroscopic Data

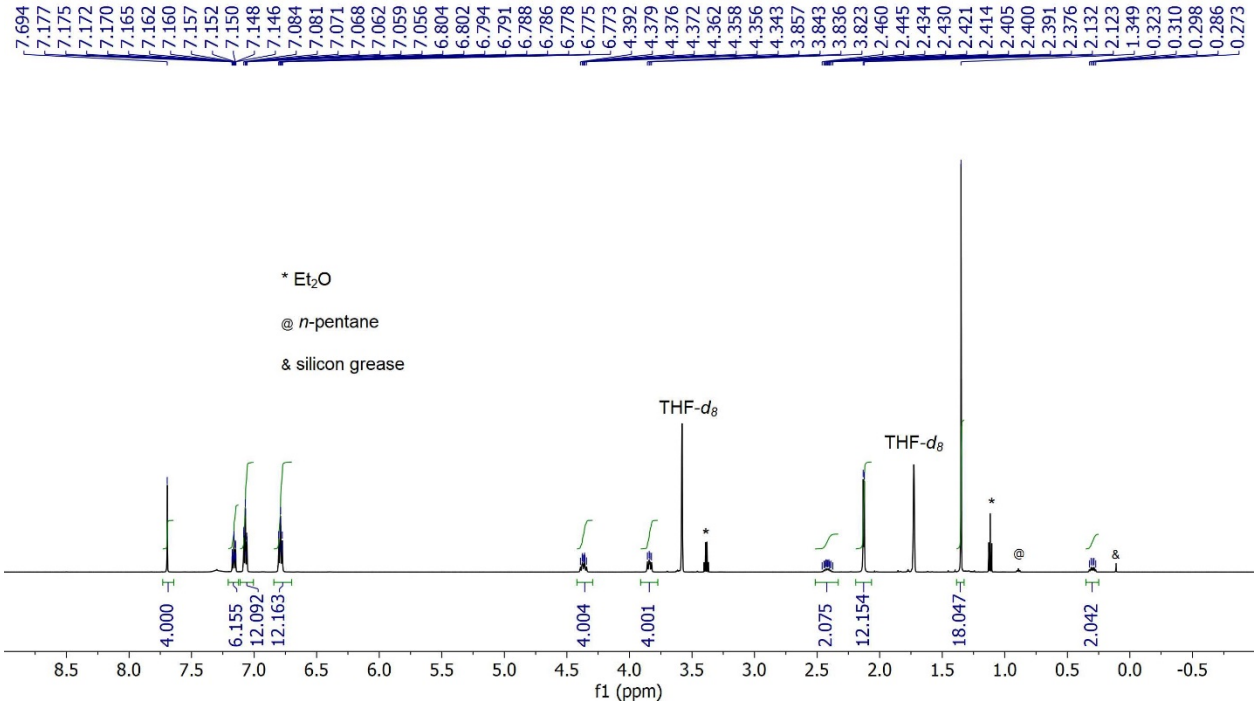


**Figure S3**. $^{1}$H NMR spectrum of $^{Ph}$**[Fe$_2$N$_2$]$^0$** in THF-$d_8$ (298 K).

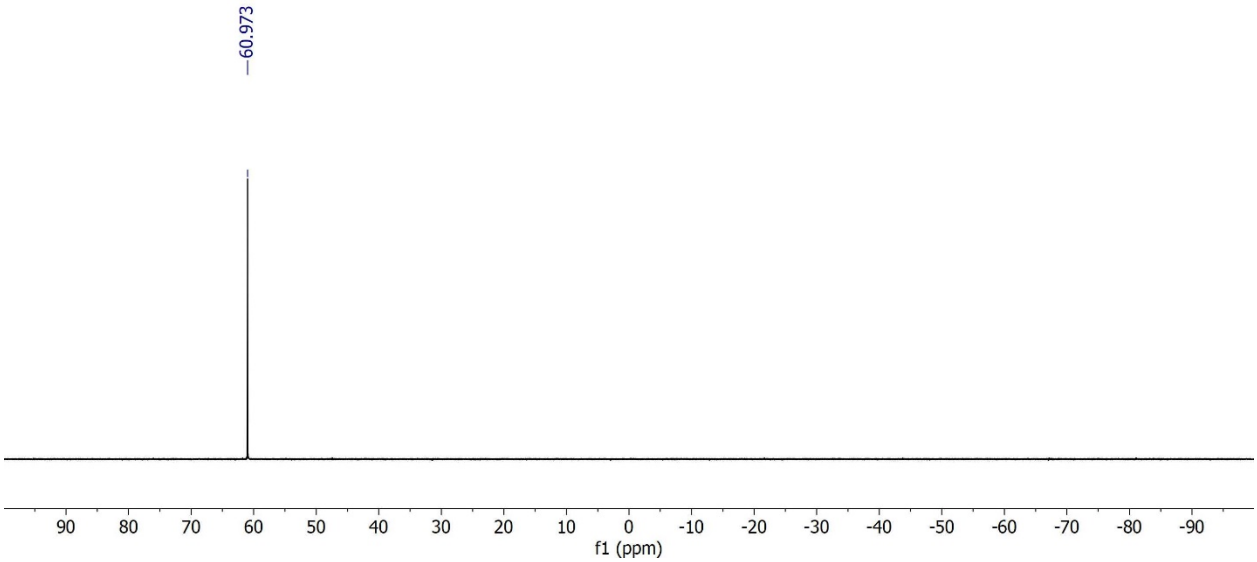


**Figure S4**. $^{31}$P{$^{1}$H} NMR spectrum of $^{Ph}$**[Fe$_2$N$_2$]$^0$** in THF-$d_8$ (298 K).

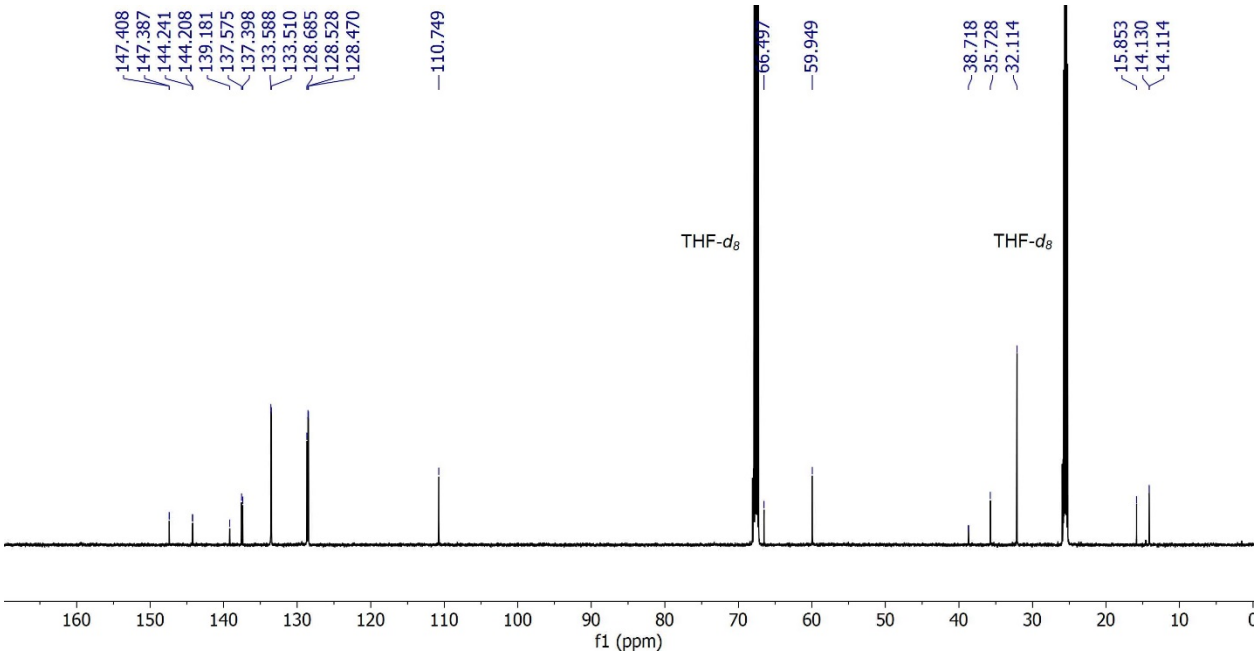


**Figure S5**. $^{13}C\{^{1}H\}$ NMR spectrum of $^{Ph}$**[Fe$_2$N$_2$]$^0$** in THF-$d_8$ (298 K).

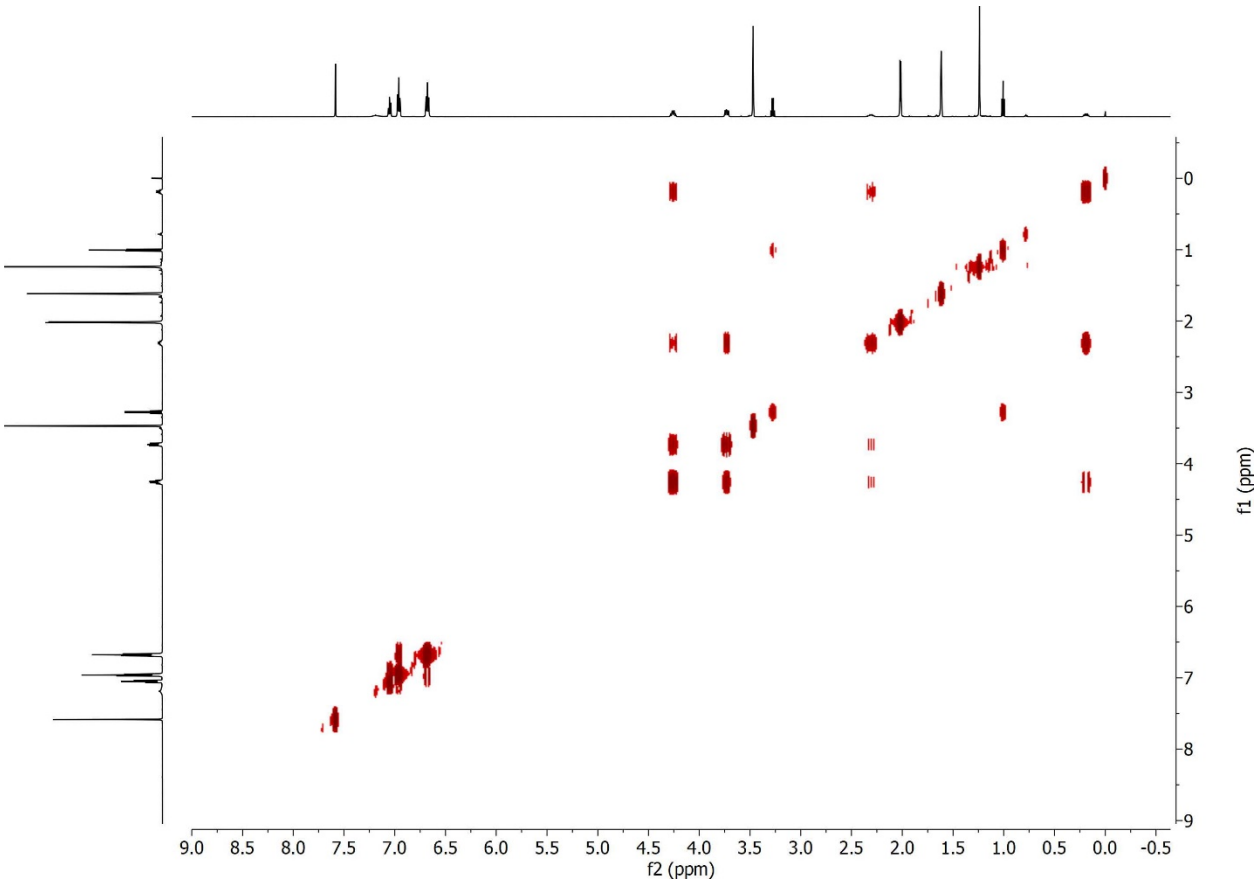


**Figure S6**. $^{1}H$-$^{1}H$ COSY NMR spectrum of $^{Ph}$**[Fe$_2$N$_2$]$^0$** in THF-$d_8$ (298 K).

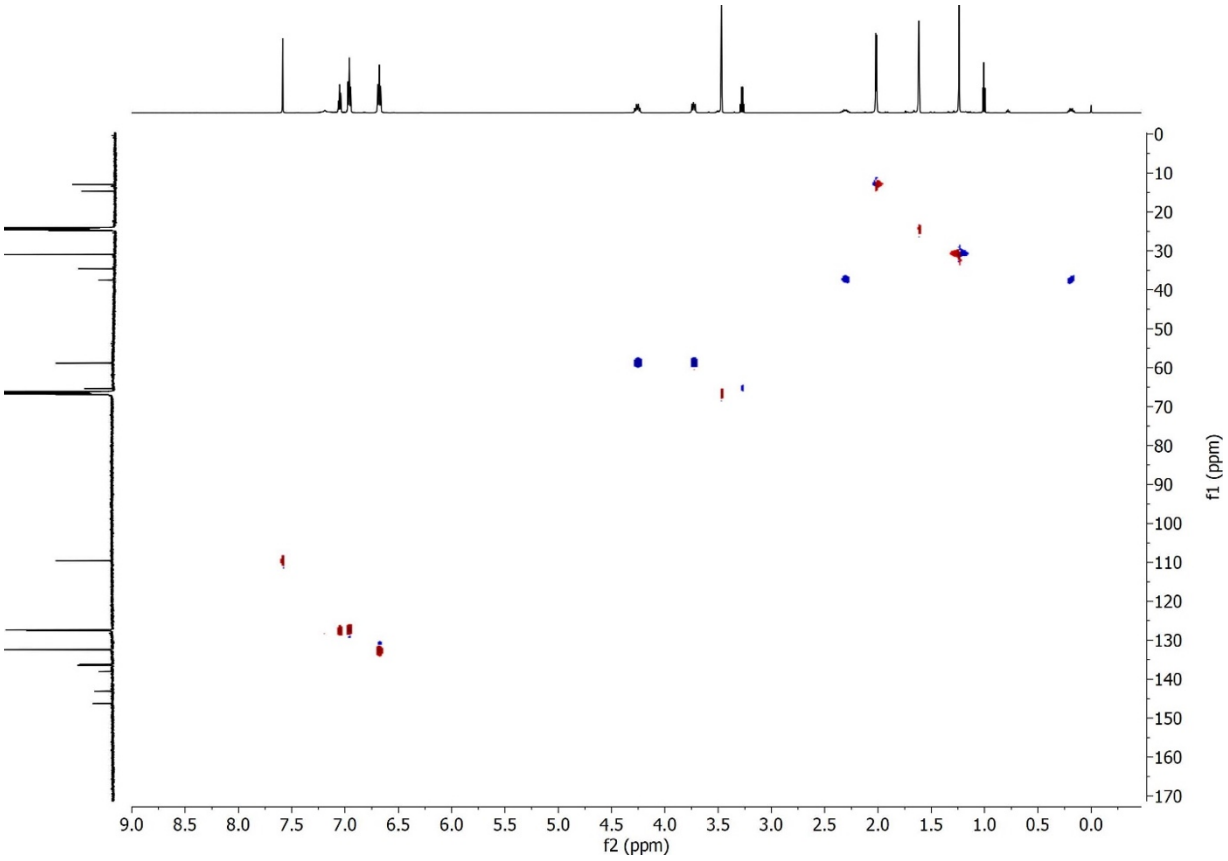


**Figure S7**. $^{1}$H-$^{13}$C HSQC NMR spectrum of $^{Ph}$**[Fe$_2$N$_2$]$^0$** in THF-$d_8$ (298 K).

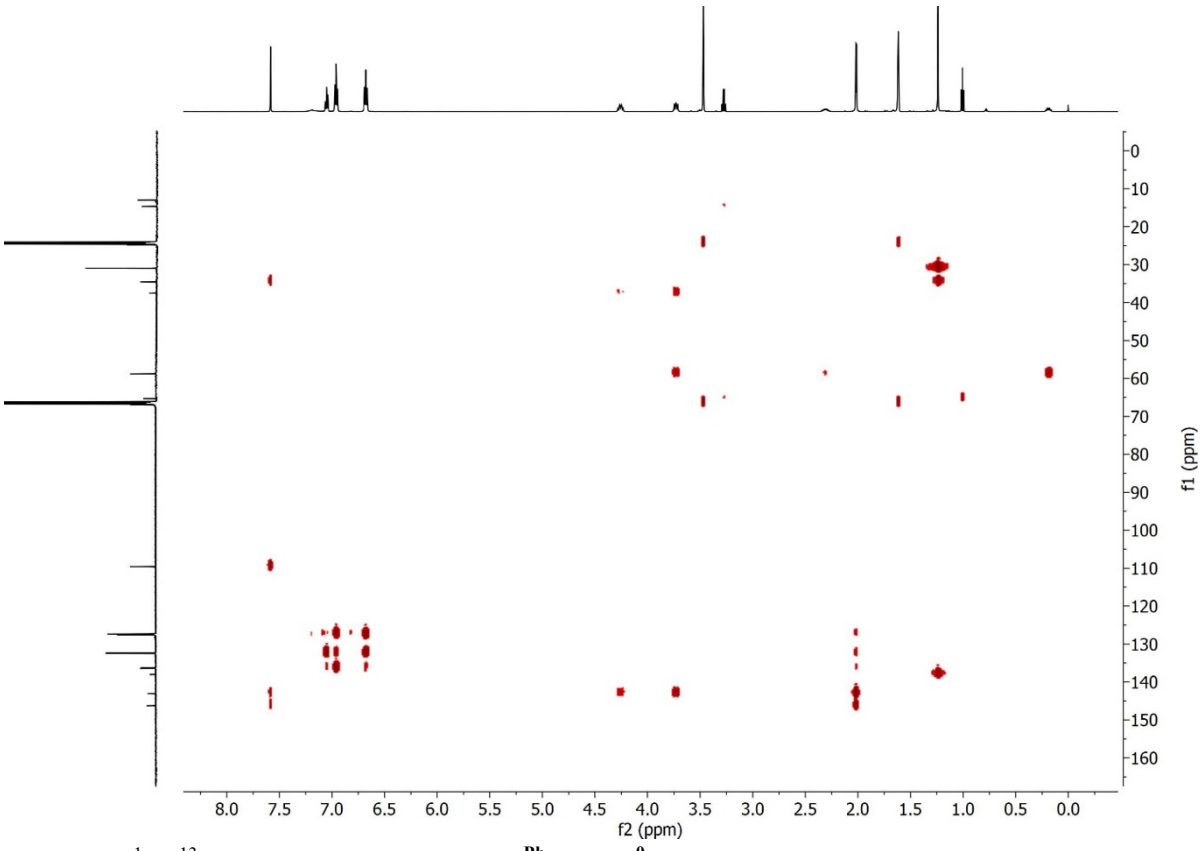


**Figure S8**. $^{1}$H–$^{13}$C HMBC NMR spectrum of $^{Ph}$**[Fe$_2$N$_2$]$^0$** in THF-$d_8$ (298 K).

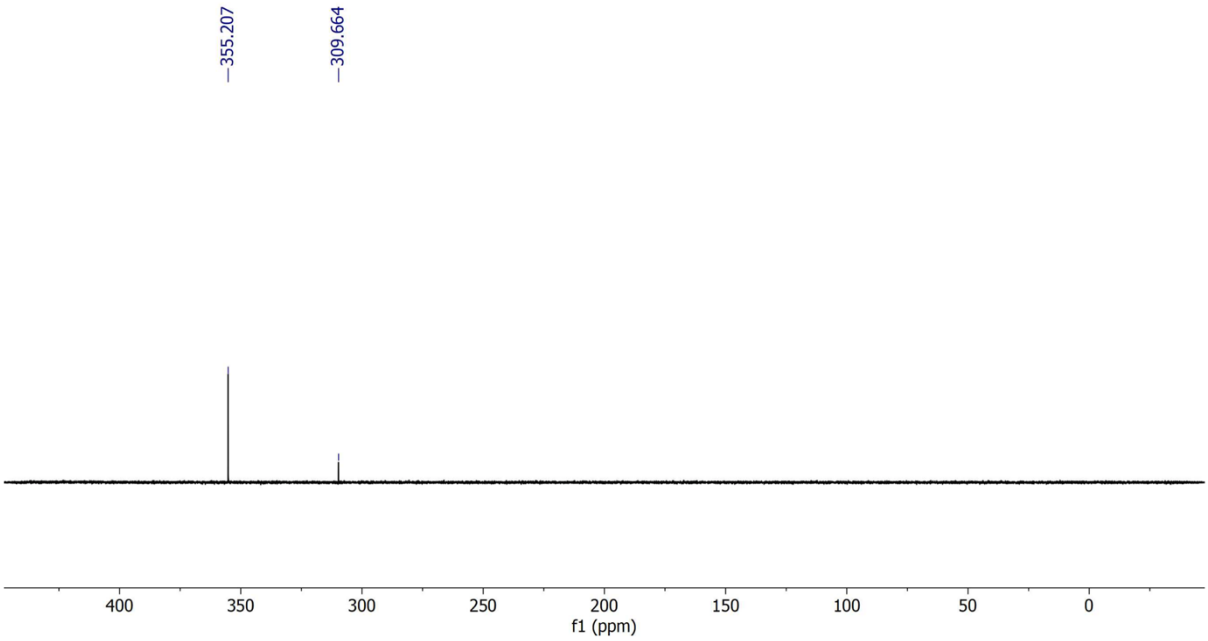


**Figure S9**. $^{15}N$ NMR spectrum of $^{Ph}[Fe_2{}^{15}N_2]^0$ in THF-$d_8$ (298 K). The feature at 309.7 ppm was tentatively assigned as free $^{15}N_2$.[15]

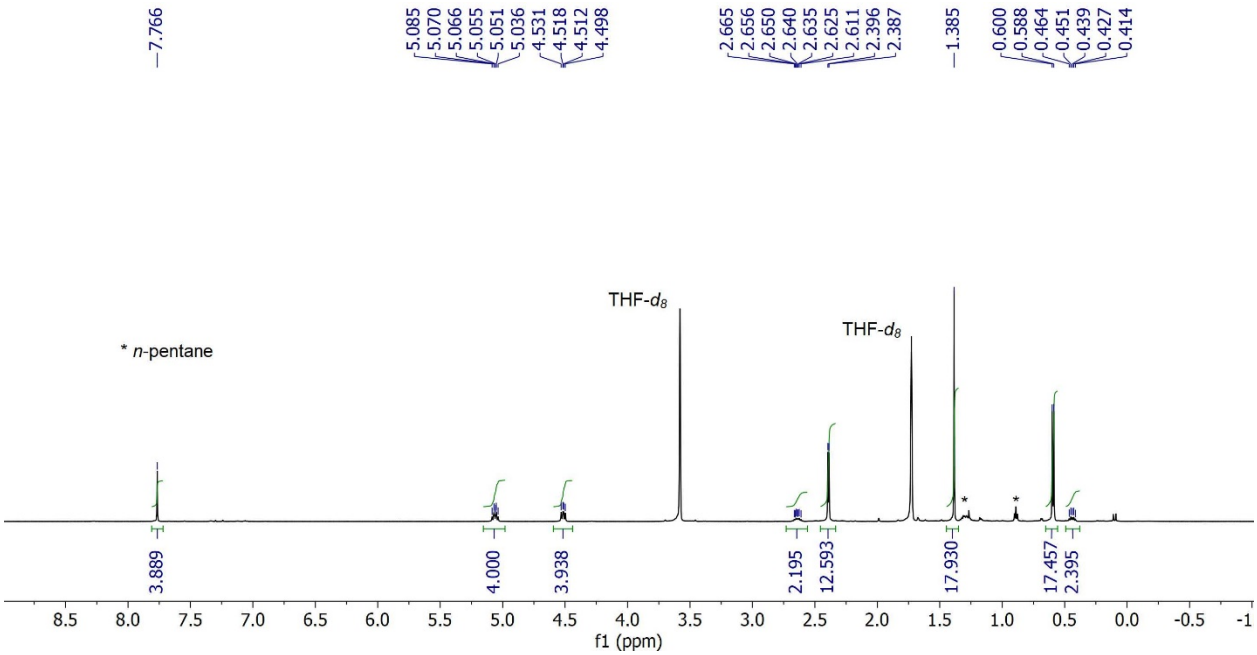


**Figure S10**. $^1H$ NMR spectrum of $^{Me}[Fe_2N_2]^0$ in THF-$d_8$ (298 K).

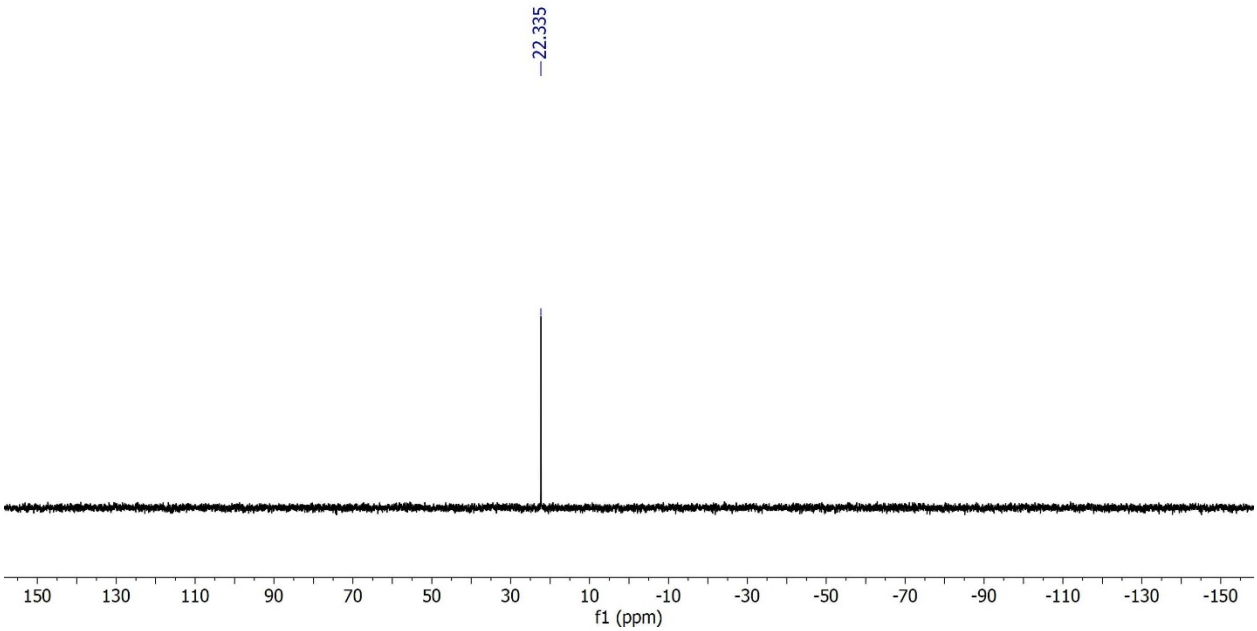


**Figure S11**. $^{31}P\{^{1}H\}$ NMR spectrum of $^{Me}[Fe_2N_2]^0$ in THF-$d_8$ (298 K).

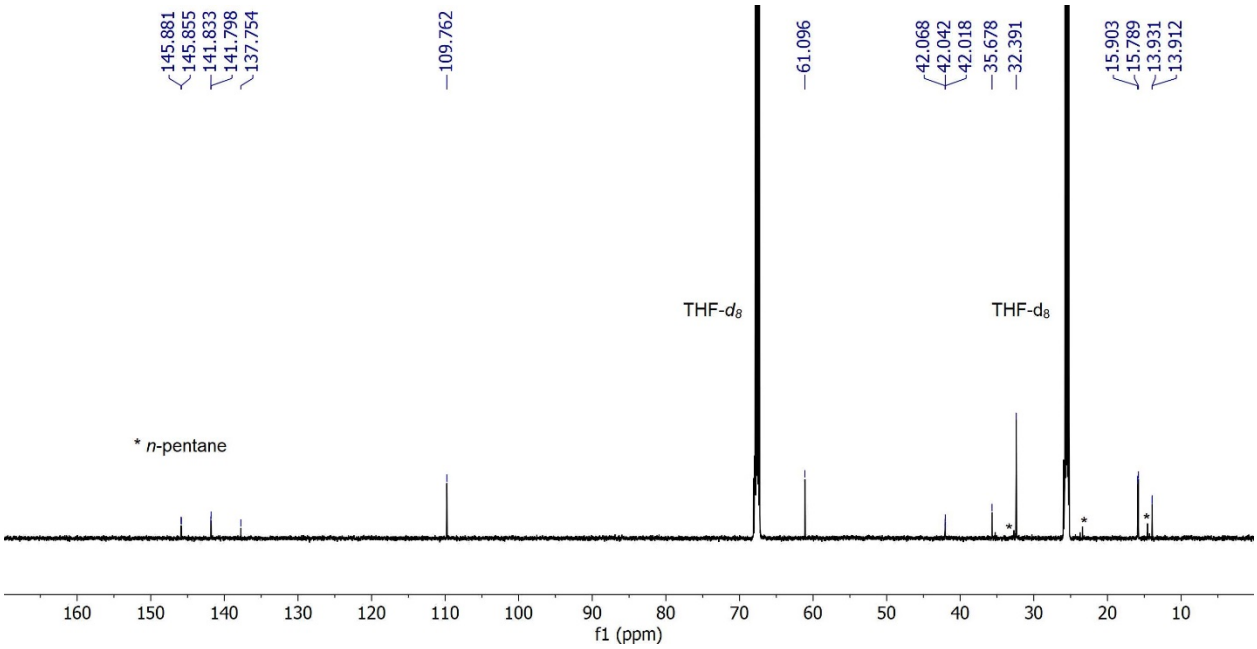


**Figure S12**. $^{13}C\{^{1}H\}$ NMR spectrum of $^{Me}[Fe_2N_2]^0$ in THF-$d_8$ (298 K).

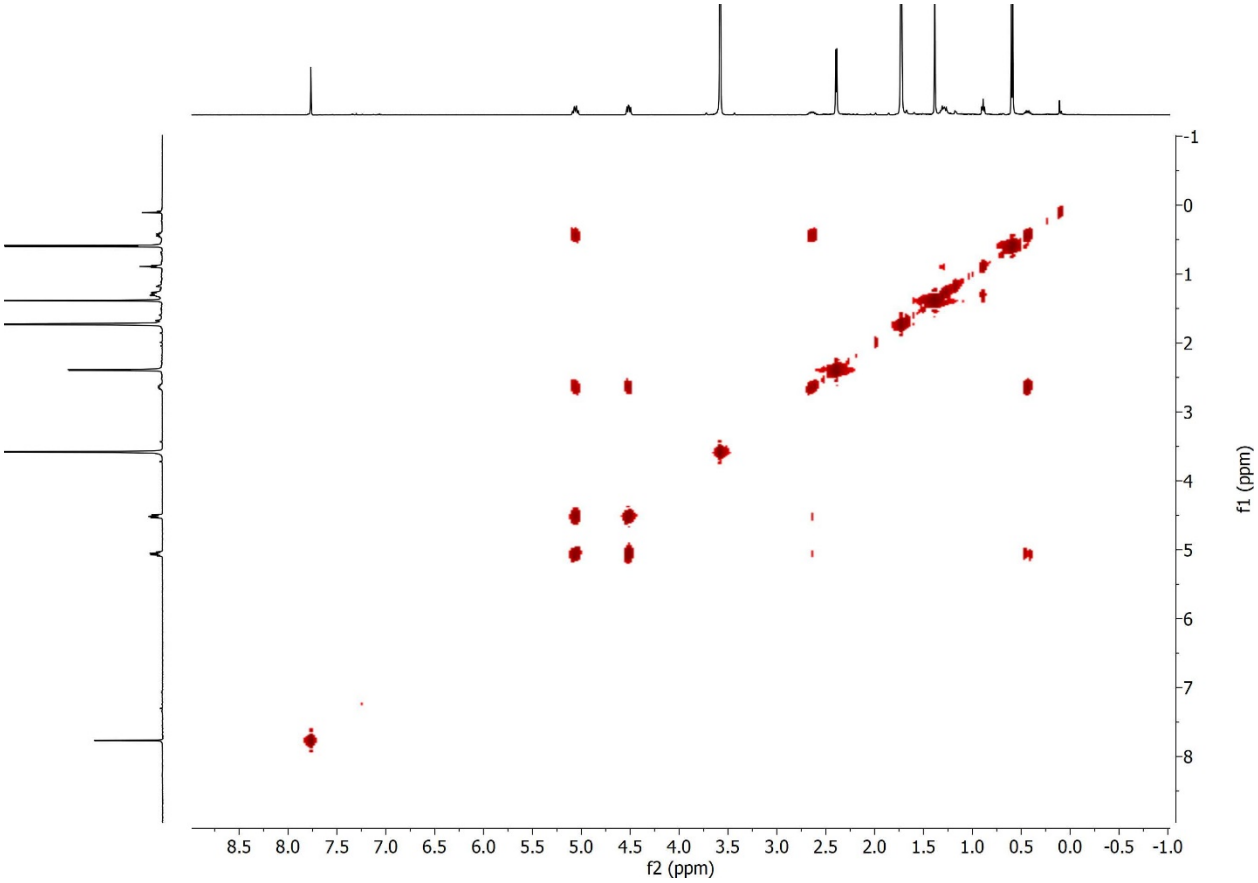


**Figure S13**. $^{1}$H–$^{1}$H COSY NMR spectrum of $^{Me}[Fe_2N_2]^0$ in THF-$d_8$ (298 K).

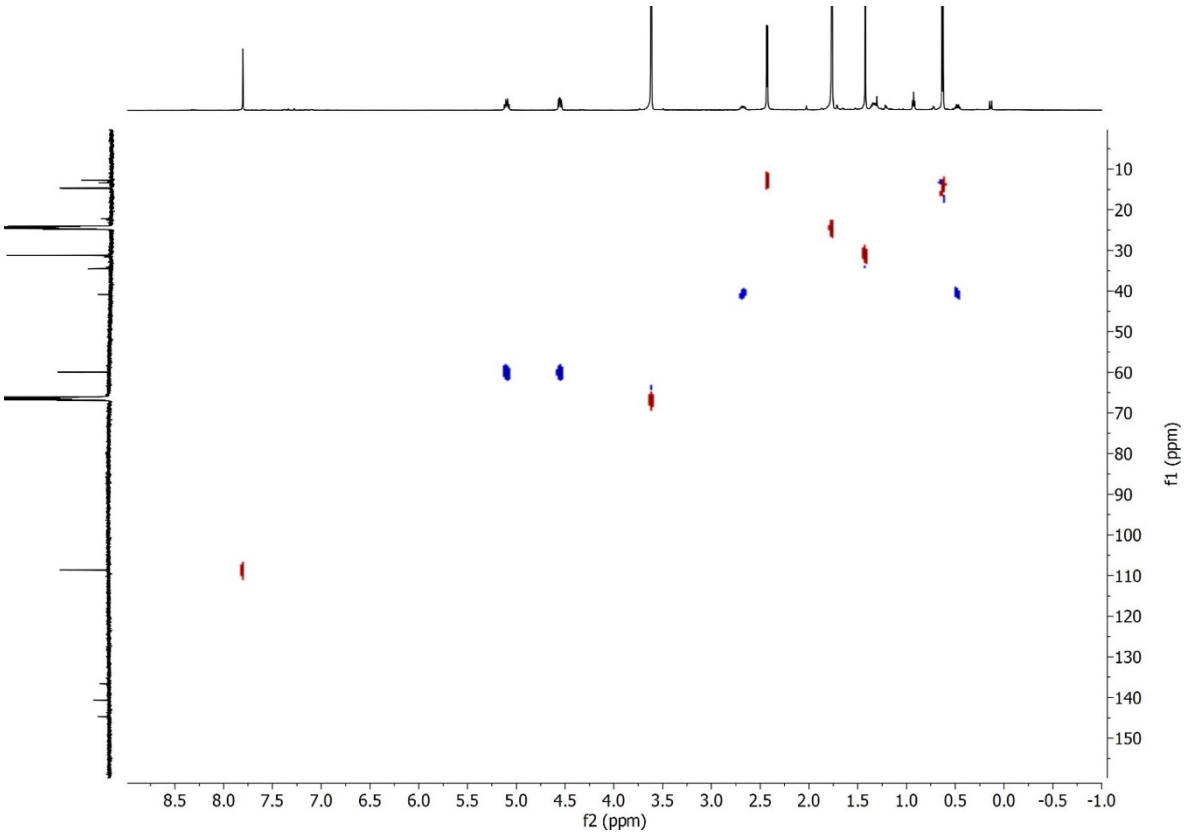


**Figure S14**. $^{1}$H–$^{13}$C HSQC NMR spectrum of $^{Me}[Fe_2N_2]^0$ in THF-$d_8$ (298 K).

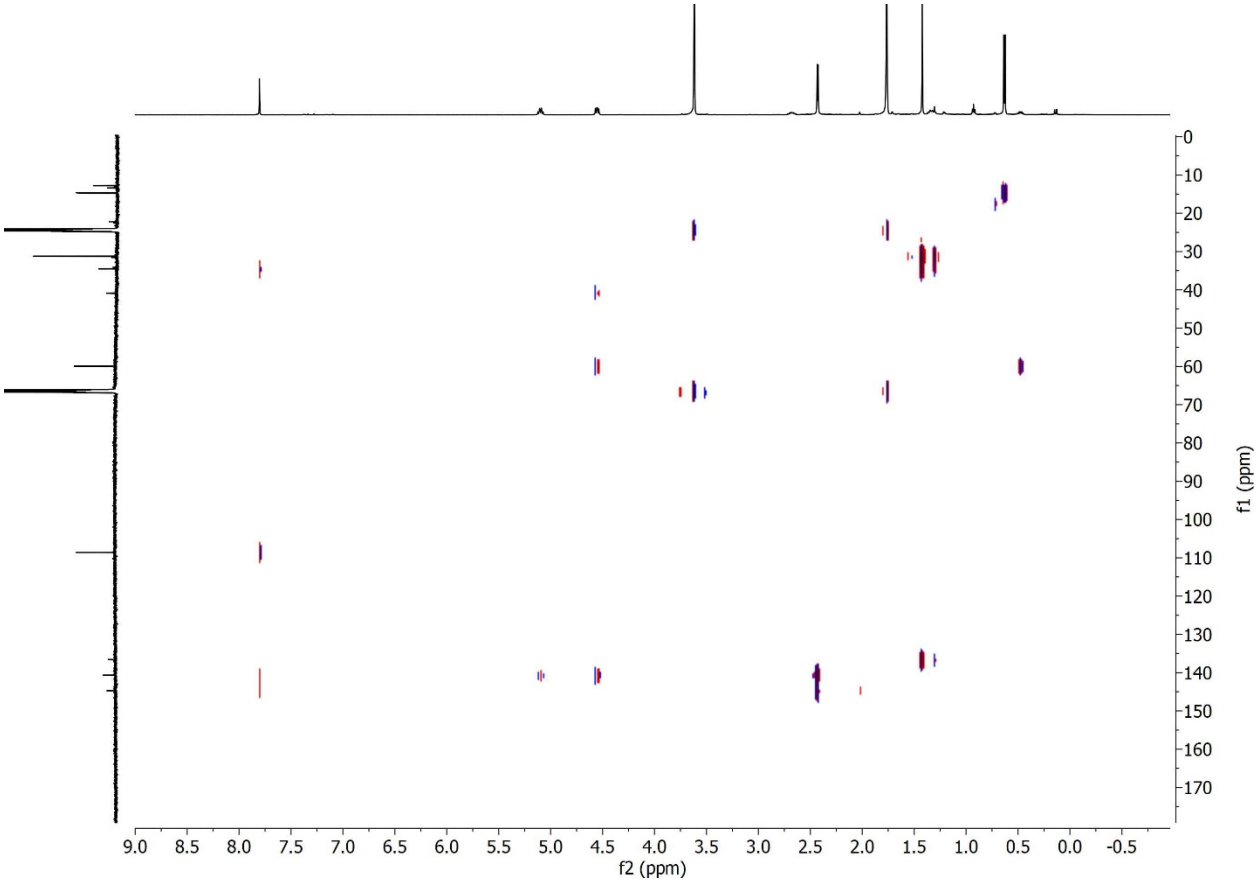


**Figure S15**. $^{1}H–^{13}C$ HMBC NMR spectrum of $^{Me}[Fe_2N_2]^0$ in THF-$d_8$ (298 K).

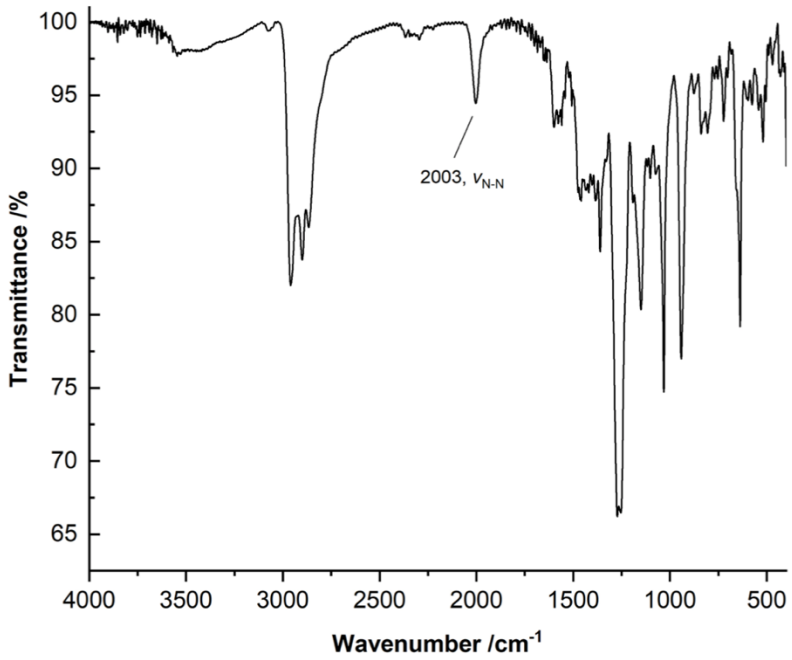

**Figure S16**. FT-IR spectra of $^{Me}[Fe_2N_2]^0$ (KBr pellet).

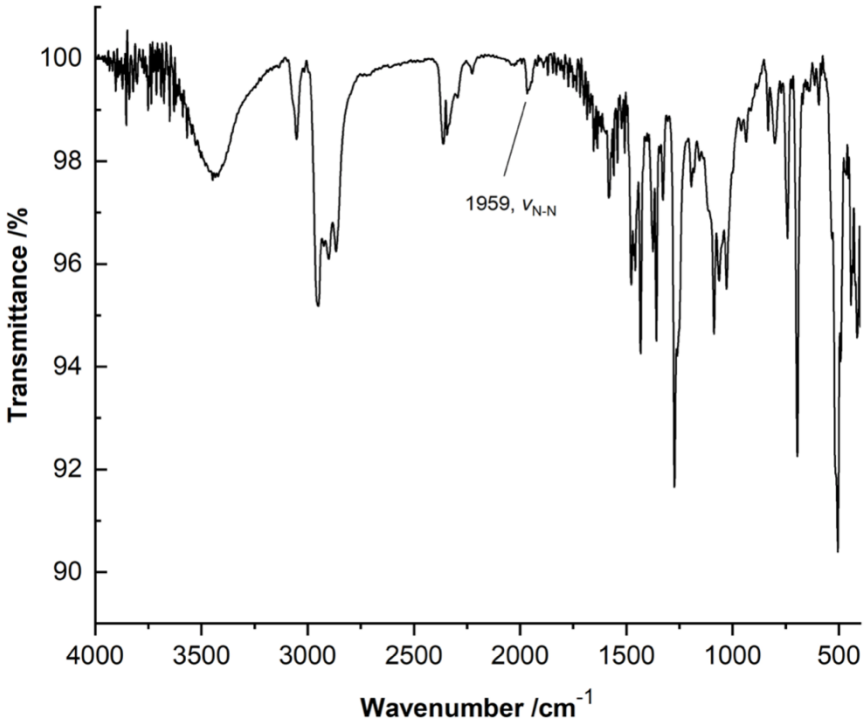


**Figure S17**. FT-IR spectra of $^{Ph}[Fe_2N_2]^0$ (KBr pellet).

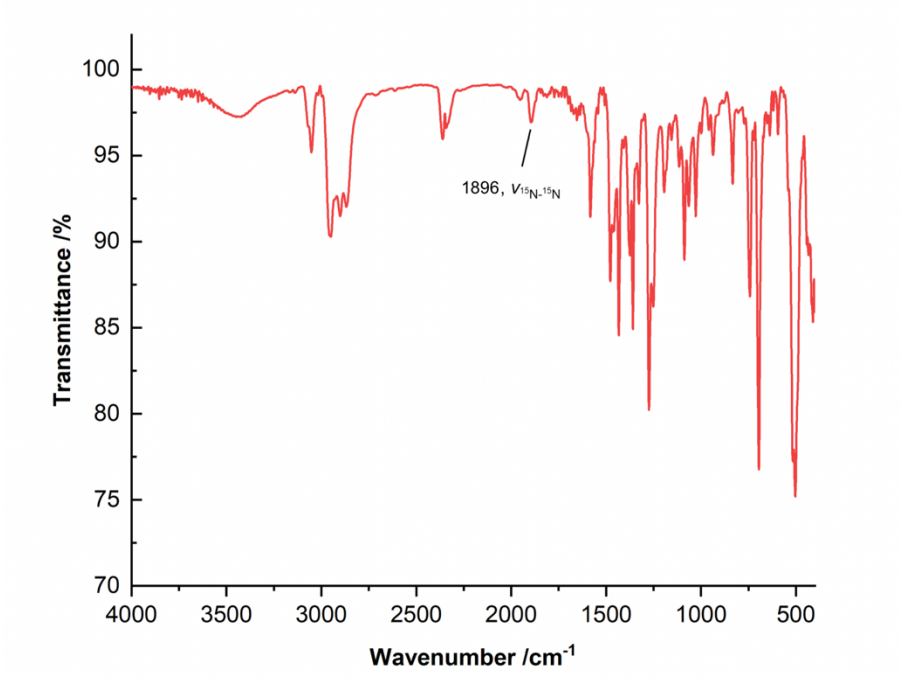


**Figure S18**. FT-IR spectra of $^{Ph}[Fe_2{}^{15}N_2]^0$ (KBr pellet).

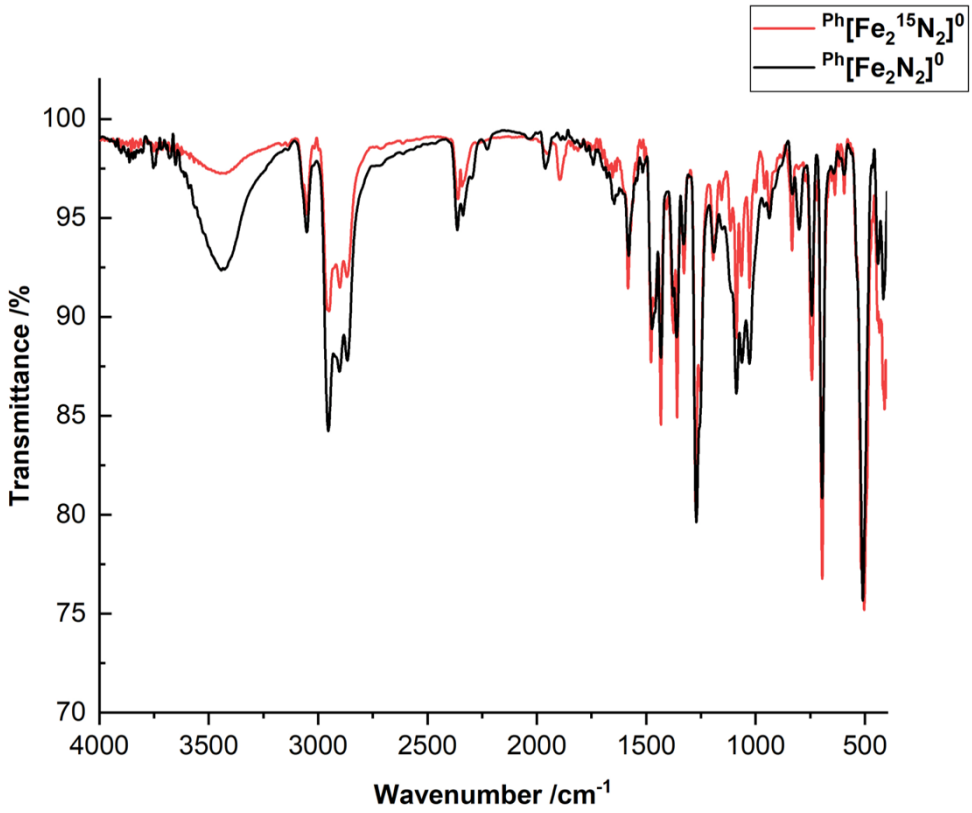


**Figure S19**. Overlay of the FT-IR spectra of $^{Ph}[Fe_2N_2]^0$ (black line) and $^{Ph}[Fe_2{}^{15}N_2]^0$ (red line).

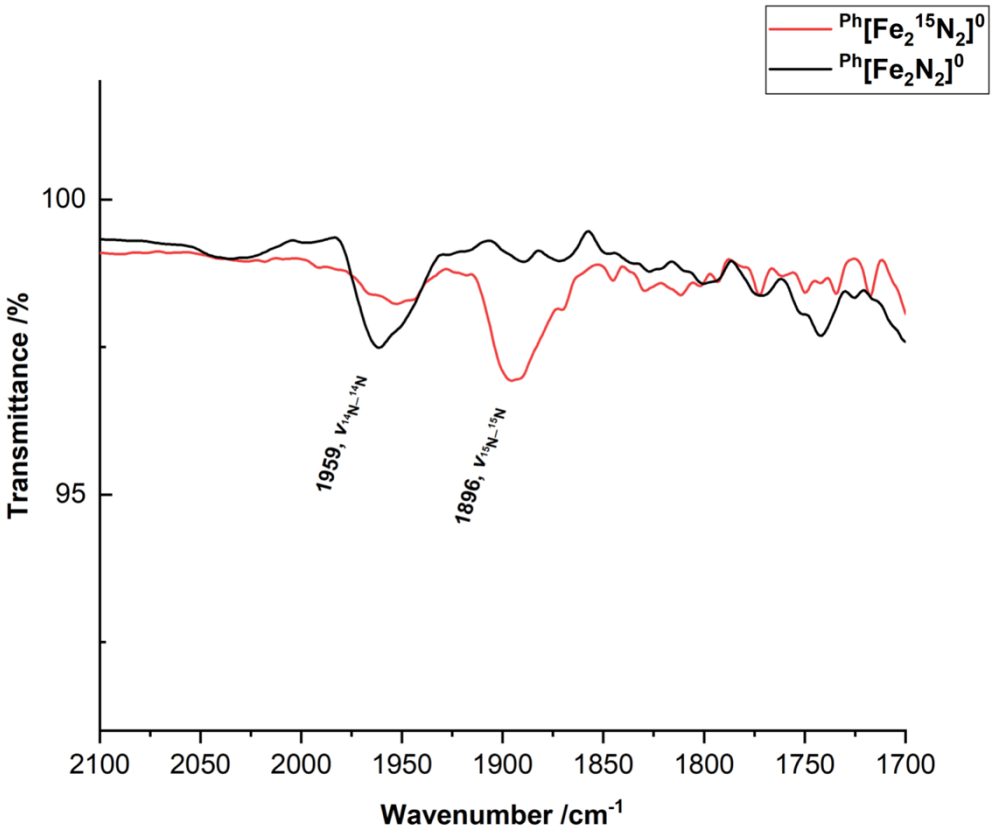


**Figure S20**. Selected region of the FT-IR spectra of $^{Ph}[Fe_2N_2]^0$ (black line) and $^{Ph}[Fe_2{}^{15}N_2]^0$ (red line).

## Electrochemistry Data

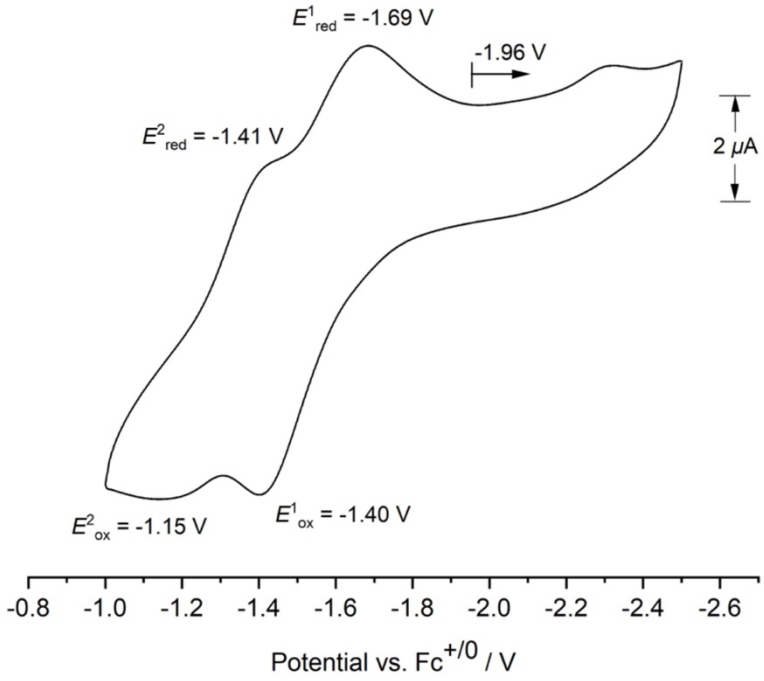


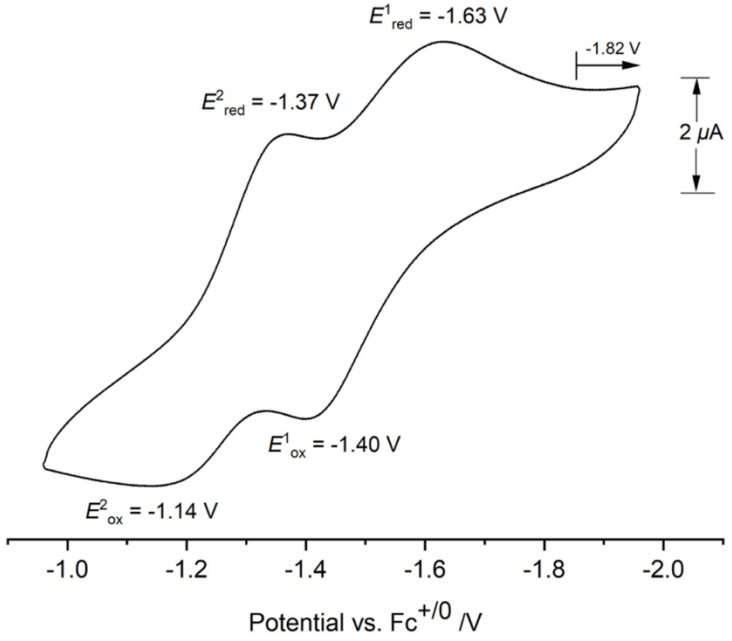


**Figure S21**. Cyclic voltammograms of $^{Ph}$**[Fe$_2$N$_2$]$^0$** (1 mM in THF), using a glassy carbon (3 mm outer diameter) working electrode, a platinum wire counter electrode, a $AgPF_6$ (100 mM in THF)/Ag reference electrode and 100 mM [$^n$Bu$_4$N][$PF_6$] as the supporting electrolyte. Scan rate 100 mV/s in THF versus $Cp_2Fe^{+/0}$. The plots show one trace from multi-cycle sweeps.

## Computational Results

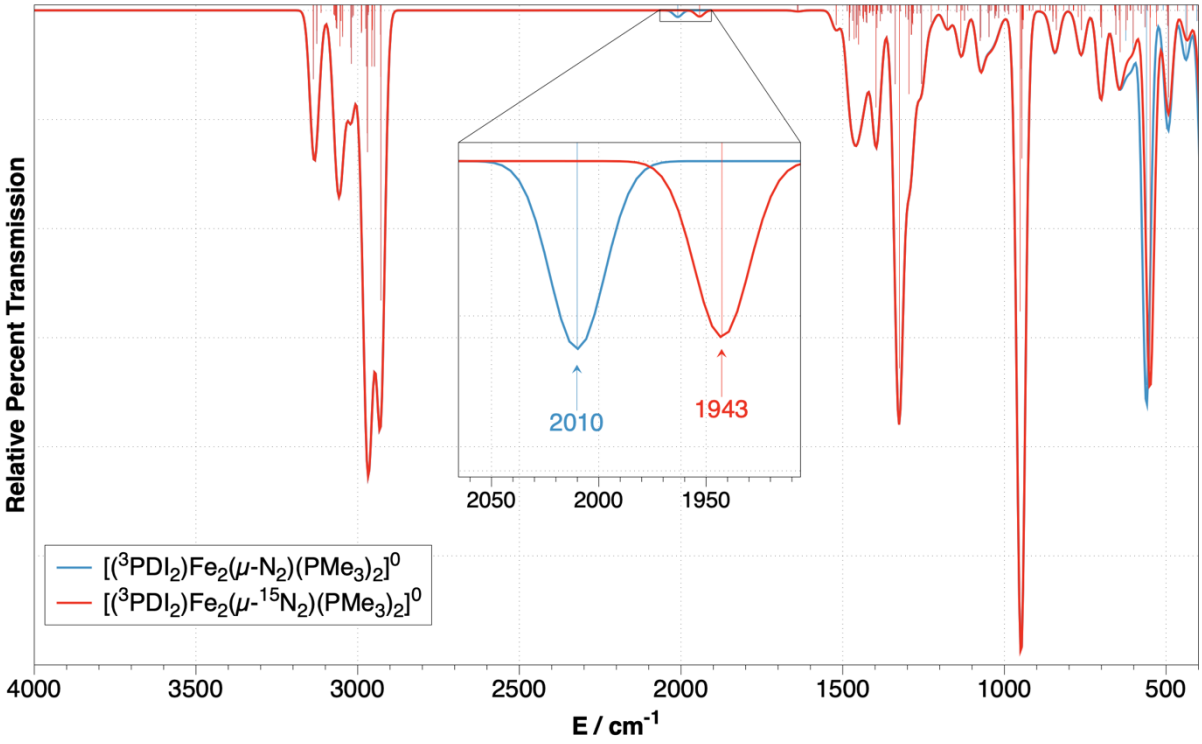


**Figure S22.** Calculated IR spectra of the truncated versions of $^{Me}[Fe_2N_2]^0$ (red) and $^{Me}[Fe_2{}^{15}N_2]^0$ (blue).

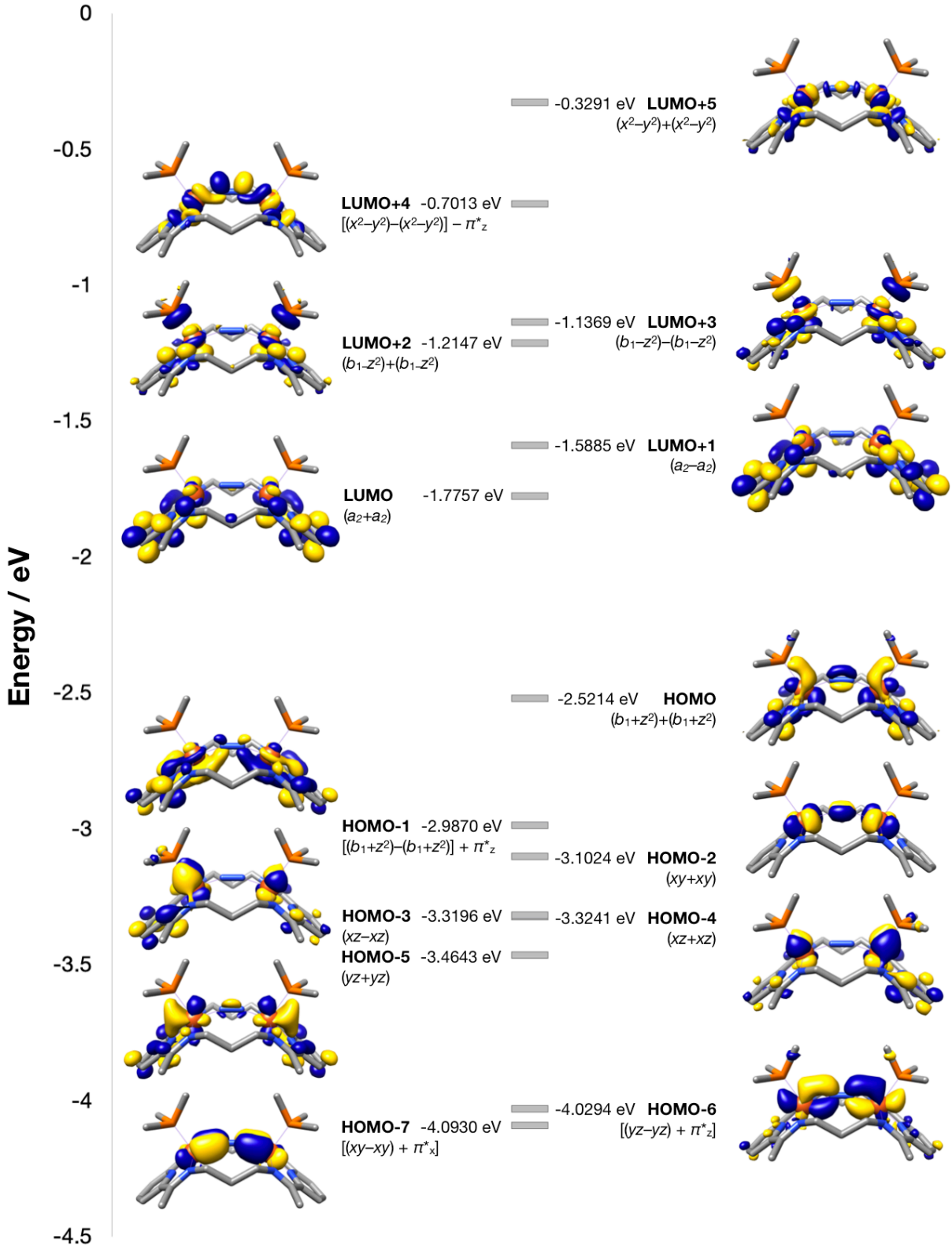


**Figure S23.** Quantitative molecular orbital diagram for the truncated version of $^{Me}[Fe_2N_2]^0$.

## DFT-optimized Atomic Coordinates

$[(^3PDI_2)Fe_2(\mu\text{-}N_2)(PMe_3)_2]^0$ ($^{Me}$**[Fe$_2$N$_2$]$^0$**)

G° = -4819.11560066 $E_h$

| | | | |
|---|---|---|---|
| Fe | 0.00514284296710 | 0.02626930822387 | 0.14266483149390 |
| Fe | -0.06816894117977 | 4.56167826172399 | 0.16344805053431 |
| P | -0.37018056654390 | -1.16330925522904 | 1.88112467407858 |
| P | -0.47469736751201 | 5.72651294470157 | 1.91173453749653 |
| N | -0.15841655019757 | 1.71516593522101 | 0.74967440405158 |
| N | -0.17741815081335 | 2.86292081967652 | 0.75599841771712 |
| N | 0.31598104977411 | -1.29278642517028 | -1.12772225131666 |
| N | -1.76206253859371 | -0.05979170020905 | -0.70628376569397 |
| N | 1.96815135809168 | -0.00165393822731 | 0.14483464317672 |
| N | 0.19724741174357 | 5.89944884805212 | -1.09739233402911 |
| N | -1.83993880282515 | 4.59714534105396 | -0.68211816186483 |
| N | 1.89210219001449 | 4.65111376962551 | 0.16089771780160 |
| C | -0.76647833438930 | -1.82134262333615 | -1.83454063357159 |
| C | 1.61251231457268 | -1.78614439245016 | -1.28882637459707 |
| C | -2.80366830220681 | 0.94179776265226 | -0.44136336243493 |
| H | -2.76622452159615 | 1.15603114822899 | 0.64315825811725 |
| H | -3.81842369762358 | 0.55447493481696 | -0.65974735573477 |
| C | 1.02158882195223 | -2.26383131998319 | 2.37236664902976 |
| H | 1.36171012384152 | -2.82374531072882 | 1.48042775749777 |
| H | 0.72928159236800 | -2.97535466733415 | 3.17081970936185 |
| H | 1.86374713481268 | -1.63819628108589 | 2.72253814060455 |
| C | 3.92967241316430 | 5.94026981895486 | -0.56746402989205 |
| H | 4.34342424740809 | 6.14841071485082 | 0.44323970329991 |
| H | 4.15472156558272 | 6.81677149427390 | -1.20124826727513 |
| H | 4.50160904909710 | 5.08202105034627 | -0.98093544881583 |
| C | -3.27574132716554 | -1.32190183303680 | -2.27417090719902 |
| H | -4.08379860584768 | -1.57324394619186 | -1.55290911025568 |
| H | -3.19387198399488 | -2.16579269006684 | -2.98256520596903 |
| H | -3.62321536099740 | -0.44091078522902 | -2.85512087639287 |
| C | 1.64945504998139 | 7.55441676902170 | -2.08791426848831 |
| H | 2.64596123735040 | 7.99293034235665 | -2.22254465857510 |
| C | -2.07263814789939 | 5.59813237102197 | -1.55714957062894 |
| C | -1.75487968384529 | -2.36342099076138 | 1.70182170718541 |
| H | -2.70251792535757 | -1.80092184994339 | 1.60815113478818 |
| H | -1.81730587034578 | -3.06039626044000 | 2.56164700532427 |
| H | -1.60634091640395 | -2.93551932389341 | 0.76644049299318 |
| C | 2.55975726942913 | -0.99379663131267 | -0.55325178729214 |
| C | -1.96135219600330 | -1.06037065786663 | -1.59005856752152 |
| C | 2.76241378282584 | 1.02761660931481 | 0.82790125103101 |

| | | | |
|---|---|---|---|
| H | 3.78121620687481 | 0.67002061186624 | 1.07631968858672 |
| H | 2.25082748092301 | 1.23720835294996 | 1.78607177321622 |
| C | 1.47709548948225 | 6.43507975102691 | -1.25738682416065 |
| C | 2.72020366991323 | 3.64356453033581 | 0.83642121313929 |
| H | 2.21658006935421 | 3.41165293348601 | 1.79366787534562 |
| H | 3.72676345436373 | 4.03311744119199 | 1.08667783134409 |
| C | 2.81965916063904 | 2.33962028991481 | -0.00460463136591 |
| H | 1.95894434856808 | 2.32818522940137 | -0.69443698486622 |
| H | 3.72917558303525 | 2.35671029415822 | -0.63931577207386 |
| C | -0.73275444312979 | 7.51905650870091 | -2.62716821126282 |
| H | -1.58632884508401 | 7.93150665414737 | -3.17917717803446 |
| C | -3.39547089799889 | 5.82266009610262 | -2.23797775339415 |
| H | -3.71328688457179 | 4.93713332897050 | -2.82895331260870 |
| H | -3.34244580849037 | 6.67679364322843 | -2.93677615899859 |
| H | -4.21089402459404 | 6.03823505197946 | -1.51352371422395 |
| C | -2.53107084928615 | 2.25948656485108 | -1.22076800582965 |
| H | -1.45615253017461 | 2.27893495765862 | -1.46678169869126 |
| H | -3.07373884221791 | 2.25572361272514 | -2.18817559653551 |
| C | 2.45062789299551 | 5.66695605568914 | -0.53057095966360 |
| C | -0.90327048939605 | 6.39906261827794 | -1.79718082215690 |
| C | 1.82239017130879 | -2.89202409711106 | -2.12865479957382 |
| H | 2.83275927891406 | -3.29722338236199 | -2.26446658759746 |
| C | -0.78691485109905 | -0.33392130289507 | 3.47348406519151 |
| H | 0.03956432326761 | 0.34985134072819 | 3.74528887045874 |
| H | -0.95558268234480 | -1.05778887700771 | 4.29716031351530 |
| H | -1.69845791026716 | 0.27608856237101 | 3.32609786736316 |
| C | -2.84758142853195 | 3.55891875742118 | -0.42739876125561 |
| H | -3.87476320559613 | 3.91449140183716 | -0.64226510861889 |
| H | -2.80385017847699 | 3.33481984959354 | 0.65490714383626 |
| C | -0.55835644638912 | -2.92780076175869 | -2.67402402163641 |
| H | -1.39706375068485 | -3.36232257607398 | -3.23183511287534 |
| C | 4.04667162769103 | -1.22040949622968 | -0.58923217728919 |
| H | 4.59210412571532 | -0.34346648622817 | -0.99934371411061 |
| H | 4.29953855237952 | -2.08752453636934 | -1.22541135677598 |
| H | 4.46546642549378 | -1.41874841326596 | 0.42131919321347 |
| C | 0.54180504126810 | 8.10134719797342 | -2.76284152609735 |
| C | 0.73443622927389 | -3.46789547049377 | -2.81150825840436 |
| C | -1.88692868745249 | 6.89562666151983 | 1.74152149273465 |
| H | -1.75229331296124 | 7.47814828903177 | 0.81049464623535 |
| H | -1.96477858157980 | 7.58452989705097 | 2.60658807642965 |
| H | -2.82165205877490 | 6.31253232838160 | 1.64417994781165 |
| C | 0.89060396428296 | 6.85525158534020 | 2.41312373878995 |
| H | 1.74813123493749 | 6.24631182620101 | 2.75532452304361 |
| H | 0.58287516040722 | 7.55121097446836 | 3.21953494236735 |

| | | | |
|---|---|---|---|
| H | 1.21581254993740 | 7.43285156270072 | 1.52696426746181 |
| C | -0.87339192183877 | 4.87570874414645 | 3.49753650636520 |
| H | -1.77326319127751 | 4.24951866382872 | 3.34633099964995 |
| H | -1.05558471538578 | 5.58976158259522 | 4.32689448827893 |
| H | -0.03355253767197 | 4.20613127548001 | 3.76366196736523 |
| H | 0.67653717524116 | 8.97419438551788 | -3.41491087906524 |
| H | 0.89855019537375 | -4.33005537467601 | -3.47101365261217 |

**References**


(1) Cui, P.; Wang, Q.; McCollom, S. P.; Manor, B. C.; Carroll, P. J.; Tomson, N. C., *Angew. Chem. Int. Ed.* **2017,** *56* (50), 15979-15983.

(2) Zhang, S.; Wang, Q.; Thierer, L. M.; Weberg, A. B.; Gau, M. R.; Carroll, P. J.; Tomson, N. C., *Inorg. Chem.* **2019,** *58* (18), 12234-12244.

(3) Wang, Q.; Zhang, S.; Cui, P.; Weberg, A. B.; Thierer, L. M.; Manor, B. C.; Gau, M. R.; Carroll, P. J.; Tomson, N. C., *Inorg. Chem.* **2019**, *doi: 10.1021/acs.inorgchem.9b02339.*

(4) Schwindt, M. A.; Lejon, T.; Hegedus, L. S., *Organometallics* **1990,** *9* (10), 2814-2819.

(5) Armarego, W. L. F.; Chai, C. L. L., Chapter 4 - Purification of Organic Chemicals. In *Purification of Laboratory Chemicals (Sixth Edition)*, Armarego, W. L. F.; Chai, C. L. L., Eds. Butterworth-Heinemann: Oxford, **2009**; pp 88-444.

(6) M. L. Luetkens, A. P. Sattelberger, H. H. Murray, J. D. Basil, J. P. Fackler, R. A. Jones, D. E. Heaton, in Inorg. Synth., Vol. 28 (Ed.: R. J. Angelici), John Wiley & Sons, Inc., New York, **1990**, pp. 305-310.

(7) CrysAlisPro 1.171.40.53: Rigaku Oxford Diffraction, Rigaku Corporation, Oxford, UK. (2019).

(8) Bruker (2012). SAINT v8.34A. Bruker AXS Inc., M., Wisconsin, USA.

(9) SADABS v2016/2: Krause, L.; Herbst-Irmer, R.; Sheldrick, G. M.; Stalke, D., *J. Appl. Crystallogr.* **2015,** *48* (1), 3-10.

(10) SCALE3 ABSPACK v1.0.7: an Oxford Diffraction program; Oxford Diffraction Ltd: Abingdon, UK, **2005**.

(11) F. Neese, WIRES: *Comput. Mol. Sci*. **2012**, *2*, 73-78.

(12) a) S. Grimme, *J. Comput. Chem.* **2006**, *27*, 1787-1799; b) S. Grimme, J. Antony, S. Ehrlich, H. Krieg, *J. Chem. Phys.* **2010**, *132*, 154104-1-19; c) S. Grimme, S. Ehrlich, L. Goerigk, *J. Comput. Chem.* **2011**, *32*, 1456-1465.

(13) a) A. Schäfer, H. Horn, R. Ahlrichs, *J. Chem. Phys.* **1992**, *97*, 2571-2577; b) A. Schäfer, C. Huber, R. Ahlrichs, *J. Chem. Phys.* **1994**, *100*, 5829-5835; c) F. Weigend, R. Ahlrichs, *Phys. Chem. Chem. Phys.* **2005**, *7*, 3297-3305.

(14) Pettersen, E. F.; Goddard, T. D.; Huang, C. C.; Couch, G. S.; Greenblatt, D. M.; Meng, E. C.; Ferrin, T. E. UCSF Chimera—A visualization system for exploratory research and analysis. *J. Comput. Chem.* **2004,** *25*, 1605-1612.

(15) Murray, L. J.; Weare, W. W.; Shearer, J.; Mitchell, A. D.; Abboud, K. A., *J. Am. Chem. Soc.* **2014**, *136* (39), 13502-13505.

(16) Higuchi, J.; Kuriyama, S.; Eizawa, A.; Arashiba, K.; Nakajima, K.; Nishibayashi, Y., *Dalton Trans.* **2018**, *47,* 1117-1121.

(17) Sunada, Y.; Imaoka, T.; Nagashima, H., *Organometallics*, **2010**, *29* (23), 6157-6160.

(18) Saouma, C. T.; Moore, C. E.; Rheingold, A. L.; Peters, J. C., *Inorg. Chem.* **2011**, *50* (22), 11285-11287.

(19) Rose, R. P.; Jones, C.; Schulten, C.; Aldridge, S.; Stasch, A., *Chem. Eur. J.* **2008**, *14* (28), 8477-8480.

(20) Field, L. D.; Guest, R. W.; Turner, P., *Inorg. Chem.* **2010**, *49* (19), 9086-9093.

(21) Zhang, F.; Song, H.; Zhuang, X.; Tung, C.; Wang, W., *J. Am. Chem. Soc.* **2017**, *139* (49), 17775-17778.

(22) Berke, H.; Bankhardt, W.; Huttner, G.; v. Seyerl, J.; Zsolnai, L., *Chem. Ber*. **1981**, *114*, 2754-2768.
(23) Takeshita, T.; Sato, K.; Nakajima, Y., *Dalton Trans.* **2018**, *47*, 17004-17010.
(24) Kandler, H.; Gauss, C.; Bidell, W.; Rosenberger, S.; Bürgi, T.; Eremenko, I. L.; Veghini, D.; Orama, O.; Burger, P.; Berke, H., *Chem. Eur. J.* **1995**, *1* (8), 541-548.
(25) Betley, T. A.; Peters, J. C., *J. Am. Chem. Soc.* **2004**, *126* (20), 6252-6254.
(26) Gu, N. X.; Oyala, P. H.; Peters, J. C., *J. Am. Chem. Soc.* **2018**, *140* (20), 6374-6382.
(27) Sunada, Y.; Imaoka, T.; Nagashima, H., *Organometallics* **2013**, *32* (7), 2112-2120.
(28) Yu, R. P.; Darmon, J. M.; Hoyt, J.; Margulieux, G.; Turner, Z. R.; Chirik, P. J., *ACS Catal.* **2012**, *2* (8), 1760-1764.
(29) Doyle, L. R.; Hill, P. J.; Wildgoose, G. G; Ashley, A. E., *Dalton Trans.* **2016**, *45*, 7550-7554.
(30) Rudd, P. A.; Liu, Shengsi.; Gagliardi, L.; Young, V. G.; Lu, C. C., *J. Am. Chem. Soc.* **2011**, *133* (51), 20724-20727.
(31) Buscagan, T. M.; Oyala, P. H.; Peters, J. C., *Angew. Chem. Int. Ed.* **2017**, *56*, 6921.
(32) Chomitz, W. A.; Arnold, J., *Chem. Commun.* **2007**, 4797-4799.
(33) Sekiguchi, Y.; Kuriyama, S.; Eizawa, A.; Arashiba, K.; Nakajima, K.; Nishibayashi, Y., *Chem. Commun.* **2017**, *53*, 12040.
(34) Suess, D. L. M.; Peters, J., *J. Am. Chem. Soc.* **2013**, *135* (13), 4938-4941.
(35) Geri, J. B.; Shanahan, P. J.; Szymczak, N. K., *J. Am. Chem. Soc*. **2017**, *139* (16), 5952-5956.
(36) McSkimming, A.; Harman, W. H., *J. Am. Chem. Soc.* **2015**, *137* (28), 8940-8943.
(37) Smith, J. M.; Lachicotte, J. R.; Pittard, K. A.; Cundari, T. R.; Rodgers, G. L.; Rodgers, K. R.; Holland, P. L., *J. Am. Chem. Soc*. **2001**, *123* (37), 9222-9223.
(38) Hein, N. M.; Suzuki, T.; Ogawa, T.; Fryzuk, M. L., *Dalton Trans.* **2016,** *45*, 14697-14708.
(39) Cummins, D. C.; Yap, G. P. A.; Theopold, K. H., *Eur. J. Inorg. Chem.* **2016**, *15-16*, 2349-2356.
(40) Suzuki, T.; Tsutsui, Y.; Ogawa, T.; Inomata, T.; Ozawa, T.; Sakai, Y.; Fryzuk, M. D.; Masuda, H., *Inorg. Chem.* **2015**, *54* (19), 9271-9281.
(41) Hung, Y.-T.; Yap, G. P. A.; Theopold, K. H., *Polyhedron* **2019,** *157*, 381-388.
(42) Vidyaratne, I.; Scott, J.; Gambarotta, S.; Budzelaar, P. H. M., *Inorg. Chem.* **2007,** *46* (17), 7040-7049.
(43) Vidyaratne, I.; Gambarotta, S.; Korobkov, I.; Budzelaar, P. H. M., *Inorg. Chem.* **2005,** *44* (5), 1187-1189.
(44) Pun, D.; Lobkovsky, E.; Chirik, P. J., *J. Am. Chem. Soc.* **2008,** *130* (18), 6047-6054.
(45) Grunze, M.; Golze, M.; Hirschwald, W.; Freund, H.-J.; Pulm, H.; Seip, U.; Tsai, N. C.; Ertl, G.; Küppers, J., *Phys. Rev. Letters* **1984**, *53*, 850.
(46) Freund, H.-J.; Bartos, B.; Messmer, R. P., *Surf. Sci.* **1985**, *185*, 187-202.
(47) Bart, S. C.; Lobkovsky, E.; Bill, E.; Wieghardt, K.; Chirik, P. J.; *Inorg. Chem.* **2007**, *46* (17), 7055-7063.
(48) Scott, J.; Vidyaratne, I.; Korobkov, I.; Gambarotta, S.; Budzelaar, P. H. M., *Inorg. Chem.* **2008**, *47* (3), 896-911.
(49) Bart, S. C.; Lobkovsky, E.; Chirik, P. J., *J. Am. Chem. Soc.* **2004**, *126* (42), 13794-13807.
(50) Darmon, J. M.; Turner, Z. R.; Lobkovsky, E.; Chirik, P. J., *Organometallics* **2012**, *31* (6), 2275-2285.
(51) Archer, A. M.; Bouwkamp, M. W.; Cortez, M.-P.; Lobkovsky, E.; Chirik, P. J., *Organometallics* **2006**, *25* (18), 4269-4278.

(52) Stieber, S. C. E.; Milsmann, C.; Hoyt, J. M.; Turner, Z. R.; Finkelstein, K. D.; Wieghardt, K.; Debeer, S.; Chirik, P. J., *Inorg. Chem.* **2012**, *51* (6), 3770-3785.
(53) Atienza, C. C. H.; Tondreau, A. M.; Weller, K. J.; Lewis, K. M.; Cruse, R. W.; Nye, S. A.; Boyer, J. L.; Delis, J. G. P.; Chirik, P. J., *ACS Catal.* **2012**, *2* (10), 2169-2172.
(54) Russell, S. K.; Darmon, J. M.; Lobkovsky, E.; Chirik, P. J.; *Inorg. Chem.* **2010**, *49* (6), 2782-2792.
(55) Fernández, I.; Trovitch, R. J.; Lobkovsky, E.; Chirik, P. J., *Organometallics* **2008,** *27* (1), 109-118.
(56) Neate, P. G. N.; Greenhalgh, M. D.; Brennessel, W. W.; Thomas, S. P.; Neidig, M. L., *J. Am. Chem. Soc.* **2019**, *141* (25), 10099-10108.
(57) Tondreau, A. M.; Milsmann, C.; Patrick, A. D.; Hoyt, H. M.; Lobkovsky, E.; Wieghardt, K.; Chirik, P. J., *J. Am. Chem. Soc.* **2010,** *132* (42), 15046-15059.
(58) Betley, T. A.; Peters, J. C., *J. Am. Chem. Soc.* **2003**, *125* (36), 10782-10783.
(59) McWilliams, S. F.; Bunting, P. C.; Kathiresan, V.; Mercado, B. Q.; Hoffman, B. M.; Long, J. R.; Holland, P. L., *Chem. Commun.*, **2018**, *54*, 13339-13342.
(60) McWilliams, S. F.; Bill, E.; Lukat-Rodgers, G.; Rodgers, K. R.; Mercado, B. Q.; Holland, P. L., *J. Am. Chem. Soc.* **2018**, *140* (27), 8586-8598.
(61) Grubel, K.; Brennessel, W. W.; Mercado, B. Q.; Holland, P. L., *J. Am. Chem. Soc.* **2014**, *136* (48), 16807-16816.
(62) Smith, J. M.; Lachicotte, J. R.; Pittard, K. A.; Cundari, T. R.; Rodgers, G. L.; Rodgers, K. R.; Holland, P. L., *J. Am. Chem. Soc*. **2001**, *123* (37), 9222-9223.
(63) McWilliams, S. F.; Rodgers, K. R.; Lukat-Rodgers, G.; Mercado, B. Q.; Grubel, K.; Holland, P. L., *Inorg. Chem.* **2016**, *55* (6), 2960-2968.